AD A065319

DDC FILE COPY

SDAC-TR-77-11

LEVEL II

A STUDY OF AMPLITUDE VARIATIONS AND m_b BIAS AT LASA SUBARRAYS

DDC
RECEIVED
MAR 6 1979
C

A.C. CHANG & D.H. VON SEGGERN

Seismic Data Analysis Center

Teledyne Geotech, 314 Montgomery Street, Alexandria, Virginia 22314

01 MAY 1978

APPROVED FOR PUBLIC RELEASE; DISTRIBUTION UNLIMITED.

Sponsored by

The Defense Advanced Research Projects Agency (DARPA)

ARPA Order No. 2551

Monitored By

AFTAC/VSC

312 Montgomery Street, Alexandria, Virginia 22314

79 03 02 036

Disclaimer: Neither the Defense Advanced Research Projects Agency nor the Air Force Technical Applications Center will be responsible for information contained herein which has been supplied by other organizations or contractors, and this document is subject to later revision as may be necessary. The views and conclusions presented are those of the authors and should not be interpreted as necessarily representing the official policies, either expressed or implied, of the Defense Advanced Research Projects Agency, the Air Force Technical Applications Center, or the US Government.

Unclassified

SECURITY CLASSIFICATION OF THIS PAGE (When Data Entered)

REPORT DOCUMENTATION PAGE	READ INSTRUCTIONS BEFORE COMPLETING FORM
1. REPORT NUMBER: SDAC-TR-77-11	2. GOVT ACCESSION NO. (mb sub b) 3. RECIPIENT'S CATALOG NUMBER
4. TITLE (and Subtitle): A STUDY OF AMPLITUDE VARIATIONS AND m_b BIAS AT LASA SUBARRAYS.	5. TYPE OF REPORT & PERIOD COVERED: Technical Rept. 6. PERFORMING ORG. REPORT NUMBER
7. AUTHOR(s): A. C. Chang, D. H. von Seggern	8. CONTRACT OR GRANT NUMBER(s): F08606-78-C-0007, VARPA Order-2551
9. PERFORMING ORGANIZATION NAME AND ADDRESS: Teledyne Geotech, 314 Montgomery Street, Alexandria, Virginia 22314	10. PROGRAM ELEMENT, PROJECT, TASK AREA & WORK UNIT NUMBERS: VT/8709
11. CONTROLLING OFFICE NAME AND ADDRESS: Defense Advanced Research Projects Agency, Nuclear Monitoring Research Office, 1400 Wilson Blvd. Arlington, Virginia 22209	12. REPORT DATE: 01 May 78; 13. NUMBER OF PAGES: 66
14. MONITORING AGENCY NAME & ADDRESS (if different from Controlling Office): VELA Seismological Center, 312 Montgomery Street, Alexandria, Virginia 22314 (12) 71 p.	15. SECURITY CLASS. (of this report): Unclassified; 15a. DECLASSIFICATION/DOWNGRADING SCHEDULE

16. DISTRIBUTION STATEMENT (of this Report)

APPROVED FOR PUBLIC RELEASE; DISTRIBUTION UNLIMITED.

17. DISTRIBUTION STATEMENT (of the abstract entered in Block 20, if different from Report)

18. SUPPLEMENTARY NOTES

Author's Report Date 10/19/77

19. KEY WORDS (Continue on reverse side if necessary and identify by block number)

LASA m_b	m_b bias
Amplitude Variations	Magnitude-yield
m_b Anomalies	Seismic Attenuation
Short Period P Amplitude	P-wave Scattering

20. ABSTRACT (Continue on reverse side if necessary and identify by block number)

LASA subarray amplitude anomalies are investigated using 395 medium-sized events, distributed in ten azimuthally divided sectors. Although LASA magnitudes, when averaged over all azimuths, are only slightly biased relative to NEIS magnitudes, the amount of bias varies with azimuth and subarray, suggesting that a simple station correction for m_b bias is not adequate. In addition, fluctuations among LASA subarrays are about 0.15 in standard deviation, even when these magnitudes are calibrated in sectors. Details of such →

next page

DD FORM 1 JAN 73 1473 EDITION OF 1 NOV 65 IS OBSOLETE

Unclassified

SECURITY CLASSIFICATION OF THIS PAGE (When Data Entered)

408258 03 02 036

fluctuations are explained in part by local crustal and upper-mantle heterogeneities under LASA. The amplitude anomalies are linearly related to the amount of travel-time anomalies in each sector, implying that both effects are due to crustal focussing.

Using a fixed effects model, the authors attempt to separate the cause of m_b bias into sector (azimuth) effect, subarray effect, and subarray-sector interaction. However, even this detailed modeling could not, with confidence, explain m_b bias. Using the reciprocity principle, even with a well calibrated station, a factor of two in uncertainty results for predictions of a station's amplitude for an event only 50 km away from a calibration event in a region as complex as LASA. The event magnitude uncertainty would probably be reduced by network averaging, or by a non-statistical detailed crust and mantle structure which could be analyzed by ray-tracing to remove source and receiver effects.

A STUDY OF AMPLITUDE ANOMALY AND m_b BIAS AT LASA SUBARRAYS

SEISMIC DATA ANALYSIS CENTER REPORT NO.: SDAC-TR-77-11

AFTAC Project Authorization No.:	VELA - T/8709/B/ETR
Project Title:	Seismic Data Analysis Center
ARPA Order No.:	2551
Name of Contractor:	TELEDYNE GEOTECH
Contract No.:	F08606-78-C-0007
Date of Contract:	01 October 1977
Amount of Contract:	$2,674,245
Contract Expiration Date:	30 September 1978
Project Manager:	Robert R. Blandford (703) 836-3882

P. O. Box 334, Alexandria, Virginia 22313

APPROVED FOR PUBLIC RELEASE; DISTRIBUTION UNLIMITED.

ABSTRACT

LASA subarray amplitude anomalies are investigated using 395 medium-sized events, distributed in ten azimuthally divided sectors. Although LASA magnitudes, when averaged over all azimuths, are only slightly biased relative to NEIS magnitudes, the amount of bias varies with azimuth and subarray, suggesting that a simple station correction for m_b bias is not adequate. In addition, fluctuations among LASA subarrays are about 0.15 in standard deviation, even when these magnitudes are calibrated in sectors. Details of such fluctuations are explained in part by local crustal and upper-mantle heterogeneities under LASA. The amplitude anomalies are linearly related to the amount of travel-time anomalies in each sector, implying that both effects are due to crustal focussing.

Using a fixed effects model, the authors attempt to separate the cause of m_b bias into sector (azimuth) effect, subarray effect, and subarray-sector interaction. However, even this detailed modeling could not, with confidence, explain m_b bias. Using the reciprocity principle, even with a well calibrated station, a factor of two in uncertainty results for predictions of a station's amplitude for an event only 50 km away from a calibration event in a region as complex as LASA. The event magnitude uncertainty would probably be reduced by network averaging, or by a non-statistical detailed crust and mantle structure which could be analyzed by ray-tracing to remove source and receiver effects.

TABLE OF CONTENTS

LIST OF FIGURES

LIST OF TABLES

INTRODUCTION

Earthquake P-wave amplitudes received at various stations show a range of fluctuations. Even when transformed into a logarithmic scale, earthquake magnitudes for one event are commonly observed to have standard deviations of more than one-half log unit. Commonly understood causes for magnitude fluctuations include: (1) radiation pattern of the seismic source, (2) regional effect of upper-mantle absorption, (3) local crustal structure under the station, and (4) imprecise distance-correction terms for some stations. The effect of radiation pattern is minimized when the seismic event is a single explosion source. Yet, a study of the LONGSHOT explosion (Lambert et al., 1969) showed that P-wave amplitude scatter of this explosion had a standard deviation of 0.44 m_b.

Regional variation of body wave magnitude in the United States is well established. In a recent paper Evernden (1977) gave a concise summary of past studies concerning station magnitude bias, stating that magnitude biases can be correlated with various factors such as travel-time anomalies, crustal thickness under the station, low-velocity channel in the upper mantle, high heat flow, and upper-mantle velocity structure. More specifically, Der (1976) showed that P-wave amplitudes of stations in the Eastern United States (EUS) are generally larger than those from stations in the Western United States (WUS) by a factor of 3. Also, he indicated that most of the P-wave amplitude bias can be attributed to regional upper-mantle absorption related to the existence of a low-velocity channel.

Amplitude fluctuations of 3 to 1 are fairly common when observations of an event's P waves are confined to a small area. LASA subarray amplitudes, for

---

Der, Z. A., 1976. On the existence, magnitude and causes of broad regional variations in body-wave amplitudes. SDAC-TR-76-8, Teledyne Geotech, Alexandria, Virginia 22314.

Evernden, J. F., 1977. Regional bias in magnitude versus yield measurement: Its explanation and modes of evaluation. Submitted for publication.

Lambert, D. G., D. H. von Seggern, S. S. Alexander, and G. A. Galat, 1969. The LONGSHOT experiment, Vol. 1: Basic observations and measurements, SDL Report No. 234, Teledyne Geotech, Alexandria, Virginia 22314.

example, have long been known to register fluctuations of 4 to 1 for most earthquakes. Fluctuations of 10 to 1 were also fairly common even after the LASA reconfiguration in January 1974 to a 50 km diameter. In a small instrument layout, such as LASA, the effects of radiation pattern, regional absorption, and distance correction term are nearly identical among all subarrays. Therefore, amplitude fluctuations at LASA subarrays are strongly affected by the local crustal and upper mantle structure. Note that these fluctuations are largely random and, therefore, not similar to the significant regional biases that Booth et al. (1975), Der (1976), and North (1977) developed. These authors smoothed over the random fluctuations and established the regional effects with statistical confidence.

Previous studies of LASA subarray amplitudes confirmed that local heterogeneities strongly influence the P-wave amplitudes. Chiburis and Hartenberger (1966) showed that for a typical event, signal amplitudes within a subarray vary by a factor of 3 to 4, and that signal amplitudes within the entire array also vary by a factor of 3 to 4. Klappenberger (1967a) studied the behavior of LASA signal amplitude variations showing that amplitudes of individual sensors and subarrays (phased sums) vary with an approximately log-normal distribution. However, his study of spatial correlation of amplitude anomalies (1967b) failed to show a fixed covariance among events. Such a result is expected if the underlying geology is not laterally uniform. Indeed,

---

Booth, D. C., P. D. Marshall, and J. B. Young, 1975. Long and short period amplitudes from earthquakes in the range 0° - 114°, Geophys. J. R. Astr. Soc., 39, 523-538.

North, R. G., 1977. Station magntiude bias - its determination, causes, and effects. Lincoln Laboratory, Technical Note 1977-24, Lexington, MA.

Chiburis, E. F., and R. A. Hartenberger, 1966. LASA signal and noise amplitudes for three teleseismic events, SDL Report No. 151, Teledyne Geotech, Alexandria, Virginia 22314.

Klappenberger, F. A., 1967a. Distribution of short period P-wave amplitude over LASA, SDL Reprot No. 187, Teledyne Geotech, Alexandria, Virginia, 22314.

Klappenberger, F. A., 1967b. Spatial correlation of amplitude anomalies. SDL Report No. 195, Teledyne Geotech, Alexandria, Virginia 22314.

Greenfield and Sheppard (1969) and Iyer (1971) have all presented interpretations of travel-time anomaly data showing that the crust under LASA is thinner toward the S30°E direction with a step-like structure just under the subarray A0. However, in another recent study (Aki et al., 1976), three-dimensional modeling was used. Results of this modeling suggested that such changes in crustal thickness are likely to be overestimated because the velocity structure of layers deduced from such modeling indicates that both the crust and the lower lithosphere appear to share the same anomaly pattern as the proposed Moho topography.

Whether or not crustal thickness changes abruptly, underlying crustal and upper-mantle structure both strongly influence travel-time and amplitude anomalies. The shallow structures cause local variations in travel time and amplitude observed at nearby stations, and factors lying in the deeper lithosphere may cause a regional effect.

This report, using LASA subarray data, examines whether seismic receiver amplitude anomalies and magnitude bias can be explained by regional and local effects. The study is divided into three parts. First, subarray beam amplitudes and array beam amplitudes are compared and systematic errors due to the array's operational method of magnitude estimation are evaluated. Second, subarray m_b's are compared with the NEIS m_b to evaluate azimuthal variations of Δm_b in terms of regional and local effects. Third, a statistical model is used to describe LASA Δm_b as a means of evaluating the significance of local and regional effects stemming from crustal and upper-mantle structure and to evaluate the precision of m_b recorded at a single site.

Greenfield, R. J., and R. M. Sheppard, 1969. The Moho depth variations under LASA and their effects of $dT/d\Delta$ measurements, Bull. Seism. Soc. Am., 59, 409-420.

Iyer, H. M., 1971. Variation of apparent velocity of teleseismic P-waves across the Large-Aperture Seismic Array, Montana, J. Geophys. Res., 76, (35), 8554-8567.

Aki, K., A. Christofferson, and E. S. Husebye, 1976. Three dimensional seismic structure of the lithosphere under Montana LASA, Bull. Seism. Soc. Am., 66, 501-524.

DATA

Events for this study were selected from the LASA 1974 event summary by collating with the NEIS bulletin. The year 1974 was selected to ensure relevance of the study to present systems because in late 1973 LASA was reconfigured to a smaller size. Only those events which collated with the NEIS bulletin in the m_b magnitude range of 5.0 to 5.5 were used. This m_b range limitation restricted LASA-recorded amplitudes of the selected events to between 10 and 100 millimicrons. Since LASA instruments are fixed to saturate (clip) at 350 millimicrons, this upper and lower limit forced event selected from the medium magnitude range, thus avoiding noise contamination of low-amplitude signals and non-linear instrument response of high-amplitude signals. During the analyses, some events were eliminated because of data problems or because the signal was mixed with the coda of another event, etc., yielding a final total of 395 events in this study.

These events were then grouped into 10 sectors based upon back azimuths of the events. The azimuthal range of each sector was adjusted so that the sectors were easily characterized in geophysical terms. Thus, the number of events in each sector ranges from 6 to 151. Table I lists the azimuthal range of each sector and the approximate seismic regions each sector covers. These data are also shown in Figure 1.

For each event selected, maximum peak-to-peak amplitudes and periods of the P arrival within 3 seconds of the onset on the unfiltered array beam and subarray beams from the A, B, C, and D rings were measured from waveform records in the Seismic Data Analysis Center (SDAC) event library. Chiburis and Hartenberger (1966) showed that subarray beams resulted in about 2 db of signal degradation. However, noise reduction in subarray beams is approximately 6 db with respect to individual sensors.

Magnitude biases are computed by subtracting NEIS m_b from calculated LASA m_b. NEIS reported magnitudes are rounded, not truncated, to the nearest 0.1 magnitude unit. There is some question that "small" NEIS m_b can represent the "true" magnitude because of the small number of stations (say, less than 10) reporting amplitudes for the event. However, magnitudes of moderately large events, such as those in this study's data base, are generally close to

TABLE I.

Division of Data Base Into 10 Sectors

Sector	Azimuthal Range	General Areas
1.	350.1 - 25.0	Alma Ata to Caspian Sea
2.	25.1 - 65.0	Turkey, Greece, Spain
3.	65.1 - 110.0	North and South Atlantic Ridge
4.	110.1 - 130.0	Puerto Rico
5.	130.1 - 160.0	South of Mexico to South of Chile
6.	160.1 - 210.0	Mexico, Easter Islands
7.	210.1 - 250.0	Tuamotu, Samoa, Fiji
8.	250.1 - 290.0	New Hebrides to Solomons
9.	290.1 - 325.0	Aleutians, Kurils, Japan, Marianas
10.	325.1 - 350.0	Tibet, India

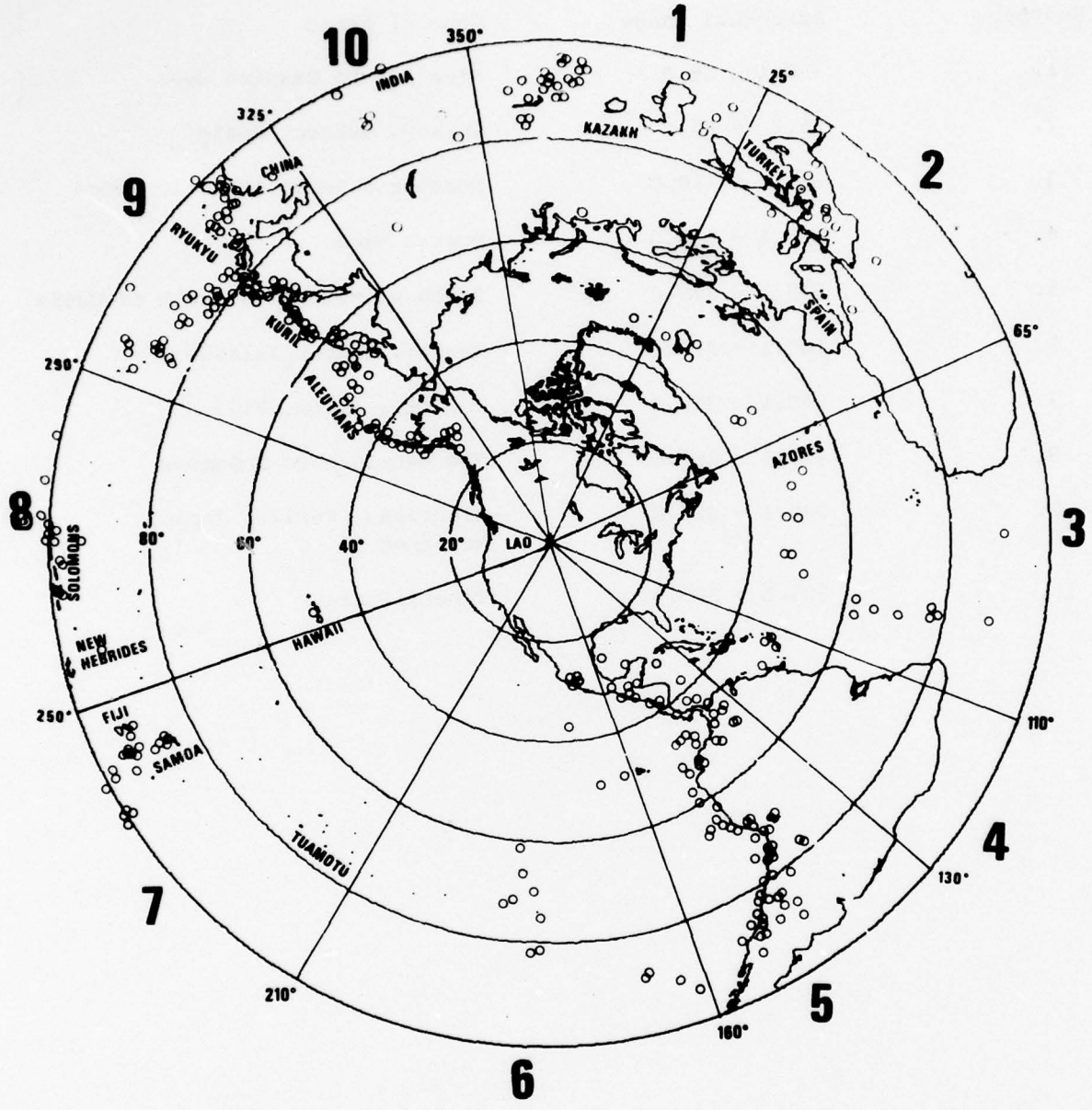

Figure 1. A world map centered at LASA to the distance of 100°, showing the division of 10 sectors in this investigation. Open circles are the locations of selected events.

true magnitudes because many stations (say, more than 10) report to NEIS and, the result of averaging many stations is to closely approximate "true" magnitudes (Husebye et al., 1974). Since a number of events are used and averaged in each sector, the effect of the NEIS bias is further reduced. The fact that some NEIS regional bias may remain is unimportant to most conclusions of this study. Exceptions to this statement are taken up as they arise.

Improper use of distance correction and use of different distance correction tables may introduce still more errors. Body wave magnitudes are computed by the formula $m_b = \log(A \cdot C/T) + B(\Delta,h)$, where A is the maximum peak-to-peak amplitude, C is the instrument correction factor, and T is the period of the signal. The $B(\Delta,h)$ factor is a distance magnitude correction factor. There are two types of B-factors available: Veith and Clawson's P-factors (1972), and Gutenberg and Richter's values known as B-(or Q-) factors for zero to peak amplitudes (converted to peak to peak by Cannon, 1967). In LASA operation all magnitudes are computed with Veith and Clawson's P-factors (1972). The difference between P-tables and Gutenberg and Richter's B-tables are as much as 0.2 magnitude unit for surface focus and they can be even greater for deeper events. In addition, two more computational errors are involved in original LASA m_b computations. The first is due to the original LASA event location which, on the average, is in error by about 1.5 degrees. Still, this error would result in only a small change in the distance-correction values. The second error is a result of LASA's failure to estimate proper depth, so a wrong correction term was used in the m_b computation. To avoid these errors, array and subarray m_b have been recomputed from the authors's own amplitude (peak-to-peak) and period measurements with the NEIS epicenter and depth and with Gutenberg-Richter B-tables, as in NEIS magnitude computations.

Husebye, E. S., A. Dahle, and K. A. Berteussen, 1974. Bias analysis of NORSAR- and ISC- reported seismic event m_b magnitudes. J. Geophys. Res., 79,(20), 2967-2978.

Veith, K. F. and G. E. Clawson, 1972. Magnitude from short-period data, Bull. Seism. Soc. Am., 62, 435-452.

Cannon, H. J., 1967. HYPOl, Technical Report 56, 106, Teledyne Geotech, Garland, Texas.

Systematic Magnitude Bias Errors

Calculating array magnitude requires first forming the array beam (phased sum), and then calculating magnitude from it. As Husebye et al. (1974) discussed, this procedure results in three types of biasing errors. The first error results from signal losses associated with array beamforming, caused by improper travel-time corrections, signal waveform difference among subarrays, and increased noise interference on subarrays compared to the full beam. Although beamforming loss, dA_{loss}, is the estimate of the reduction of array beam amplitude from the average subarray amplitude, it does not comprise the magnitude bias, because magnitudes are computed with amplitudes and periods. The second measure of error, dm_{loss}, is, therefore, the measure of deviations of the array beam A/T from the average subarray A/T. The third type of non-random error, dm_{skew}, is the difference between log(average A/T) and average log(A/T).

Because this study focuses on measurement of magnitude bias at LASA, all bias computations are taken with the following formula:

$$\Delta m_{ijk} = m_{ijk}^{LASA} - m^{NEIS} \tag{1}$$

for i-th subarray, j-th sector, k-th event. Using this formula, LASA m_b is greater than NEIS m_b if Δm_b is positive, and negative if vice-versa. Similarly, dA_{loss} and dm_{loss} are positive when array amplitudes (magnitudes) are higher than subarray averages. Therefore, the sign of these measurements are the reverse of Husebye et al.s' (1974). Finally, the total non-random m_b bias, dm_{bias}, is the sum of dm_{loss} and dm_{skew} measured in each sector. The following formulas express the relation of non-random errors measured at LASA:

$$dm_{bias} = dm_{loss} + dm_{skew} \tag{2}$$

$$dA_{loss} = \log A_B - \log \left(\frac{1}{N} \sum_{i=1}^{N} a_i \right) \tag{3}$$

$$dm_{loss} = \log\left(\frac{A_B \cdot c_B}{T_B}\right) - \log\left[\frac{1}{N}\sum_{i=1}^{N}\left(\frac{a_i \cdot c_i}{T_i}\right)\right] \qquad (4)$$

$$dm_{skew} = \log\left[\frac{1}{N}\sum_{i=1}^{N}\left(\frac{a_i \cdot c_i}{T_i}\right)\right] - \frac{1}{N}\sum_{i=1}^{N}\log\left(\frac{a_i \cdot c_i}{T_i}\right) \qquad (5)$$

where A_B is the maximum zero-to-peak amplitude of the LASA array beam, and a_i is the maximum zero-to-peak amplitude of the i-th subarray for that event. c_B and c_i are instrument response correction factors, and T_B and T_i are periods of array beam (B) and subarray beam (i) signals. By combining (4) and (5), the total dm_{bias} in (2) can be simplified as,

$$dm_{bias} = \log\left(\frac{A_B \cdot c_B}{T_B}\right) - \frac{1}{N}\sum_{i=1}^{N}\log\left(\frac{a_i \cdot c_i}{T_i}\right) \qquad (6)$$

which could have been directly written. Errors with these formulas are computed for each independent event and averaged over the events in each sector; Table II shows the results.

Unlike Husebye et al.'s (1974) evaluation of NORSAR, where each region showed $dA_{loss} < 0$, dA_{loss} for LASA shows six gains and four losses in the ten sectors. This means that A_B is slightly higher than the average of a_i, the distribution of a_i is perhaps slightly skewed, and that the loss of LASA array beamforming is very small. Similarly, dm_{loss} was such that array magnitudes were biased higher than the subarray average. Since dm_{skew} is all positive, the total magnitude bias is all positive, except in sector 2. Averaging all sectors the LASA magnitude bias is 0.038 m_b units, a figure demonstrating that systematic error at LASA is quite small.

Standard Deviations of dm_{bias} and Subarray m_b

The magnitude biases given in Table II are computed by adding two systematic losses, dm_{loss} and dm_{skew}, with formulas (4) and (5). Alternatively, dm_{bias} and deviations of dm_{bias} can both be calculated at the same time using formula (6). Thus, simplify formula (6) with the following notations:

TABLE II

LASA array beam losses and magnitude biases

for each sector calculated with equations 3, 4, 5, and 6.

Sector	Azimuth range	No. of events	Beam Loss	Magnitude Bias		
			dA_{loss}	dm_{loss}	dm_{skew}	dm_{bias}
1	350.1-25.0	35	0.089	-0.019	0.022	0.003
2	25.1-65.0	22	-0.082	-0.048	0.032	-0.016
3	65.1-110.0	16	0.153	0.038	0.034	0.072
4	110.1-130.0	6	-0.091	-0.006	0.020	0.014
5	130.1-160.0	97	-0.015	0.020	0.032	0.052
6	160.1-210.0	20	0.124	0.078	0.023	0.101
7	210.1-250.0	24	0.059	0.044	0.012	0.056
8	250.1-290.0	17	0.069	0.035	0.013	0.048
9	290.1-325.0	151	-0.072	-0.015	0.028	0.013
10	325.1-350.0	7	0.075	-0.011	0.047	0.036
AVERAGE			0.031	0.012	0.026	0.038

$$dm_{Bjk} = m_{Bjk} - m_{.jk} \qquad (6a)$$

where

dm = magnitude bias

m = magnitude

B = the array beam

j = a subscript for the sector

k = a subscript for the event

. = a subscript for the averaged value over subarrays

Each independent event is associated with a value of dm_{bias}. Thus, by averaging over the entire K events in sector J, the average dm_{bias} and error is obtained, that is

$$dm_{Bjk} = dm_{Bj.} + e_{Bjk} \qquad (7)$$

The term $dm_{Bj.}$ is the mean magnitude bias for the j-th sector, and it is equivalent to dm_{bias} shown in Table II; its standard deviation $\sigma_{Bj.}$ measures the width of the distributions.

Similarly, evaluating how subarray m_b's fluctuate from the mean can be done using the same subscript notation, let

$$m_{ijk} = m_{.jk} + e_{ijk} \qquad (8)$$

where m_{ijk} is the magnitude for the i-th subarray, j-th sector, and k-th event; and $m_{.jk}$ is the average magnitude of all subarrays. For a particular jk-th event, subarray magnitude fluctuates from the mean with a standard deviation of $\sigma_{.jk}$. Averaging over the entire k events in the j-th sector yields

$$\sigma_{.jk} = \sigma_{.j.} + e_{.jk} \qquad (9)$$

The term $\sigma_{.j.}$ is the mean standard deviation of the subarray magnitude fluctuations in the j-th sector, and $\sigma(\sigma_{.j.})$ represents the standard deviation of the term $e_{.jk}$ shown in (9). Results of these computations using (7) and (9) are shown in Table III.

Magnitude biases in the first column of Table III are almost the same as those in the last column of Table II. Although LASA m_b bias in column 1 are small (-0.031 m_b over all events-) standard deviations are in the range

TABLE III

Measurements of magnitude bias, and measurements of subarray magnitude fluctuations

Sector	Magnitude Bias		Subarray m_b Fluctuations	
	$dm_{Bj.}$	$\sigma_{Bj.}$	$\sigma_{.j.}$	$\sigma(\sigma_{.j.})$
1	0.003	0.134	0.144	0.035
2	-0.017	0.185	0.177	0.030
3	0.072	0.115	0.166	0.057
4	0.014	0.048	0.133	0.029
5	0.051	0.092	0.160	0.055
6	0.101	0.109	0.134	0.046
7	0.055	0.125	0.106	0.016
8	0.047	0.063	0.108	0.016
9	0.013	0.151	0.157	0.027
10	0.036	0.119	0.213	0.026

of 0.1 m_b which means that even if LASA m_b biases are calibrated in each sector with $dm_{Bj.}$, the accuracy of the estimates is limited by the value of $\sigma_{Bj.}$ in column 2.

Measurements of subarray magnitude fluctuations, $\sigma_{.j.}$, are in the range of 0.11 to 0.21 m_b, with average 0.15 m_b. Also, the standard deviation $\sigma(\sigma_{.j.})$ is very small in each sector, making subarray m_b fluctuations consistently in the range of 0.15 m_b. The range of subarray fluctuations -- from smallest to largest subarray would include 14 of the 16 subarrays or $\simeq$ 90% of the samples. The extreme samples would lie at $\simeq \pm 1.64\sigma$, so if $\sigma = 0.15$ then the extreme subarrays for each event would be expected to be 0.49 magnitude units apart about a factor of 3.

GEOPHYSICAL CAUSES OF MAGNITUDE BIAS

Subarray m_b Biases Compared to NEIS m_b

For events selected in a sector, the magnitude bias Δm_b is computed using (1) and then averaged over the number of events in the sector. The result includes magnitude biases for each subarray and sector, as well as associated standard deviations. These values are shown in Table IV. The last column of Table IV shows the average of Δm_b over all sectors for each subarray, $\overline{\Delta m_b}$. Magnitude biases may, of course, be due in part to NEIS regional bias.

The standard deviations of m_b biases shown in this table are generally in the range of 0.30 to 0.35. Standard deviations of all subarrays are lower in sectors 4 and 10. However, this result is suspect because only six or seven events, respectively, were analyzed in each sector. With the exception of these two sectors, the standard deviations are stable for all subarrays and sectors. Thus, while subarray magnitudes can be azimuthally calibrated, the best possible improvement are magnitude estimates with standard deviations of 0.3. This table also shows that the standard deviations of the full array (row labeled LASA) are in the same range as the subarrays, indicating that any signal estimate, array or subarray, can be azimuthally calibrated to behave like a single station while the standard deviations remain the same. If the NEIS regional bias varied from event to event, this would contribute to the variance. However since $5.0 \leq m_b \leq 5.5$ the bias would not be expected to vary much because the same suite of station would be expected to detect all events. Earthquake radiation pattern variations are presumably responsible for much of this variance. (Recall that the σ of subarray m_b relative to the mean LASA beam m_b is 0.15.)

Uniform Azimuthal Variations of Subarray Magnitude Biases -- a Regional Effect

Evernden (1977) suggested that P-wave amplitudes received at stations in a broad region can be calibrated with a regional correction. This observation suggests that one correction value, such as $\overline{\Delta m_b}$ in Table IV, applies to events from all directions. Although the array $\overline{\Delta m_b}$ is small and near the value of 0.1 in this table, azimuthal variations are much greater in all subarrays, suggesting that a simple correction is not adequate for any particular subarray. Figure 2 shows the plot of Δm_b against azimuth for all sub-

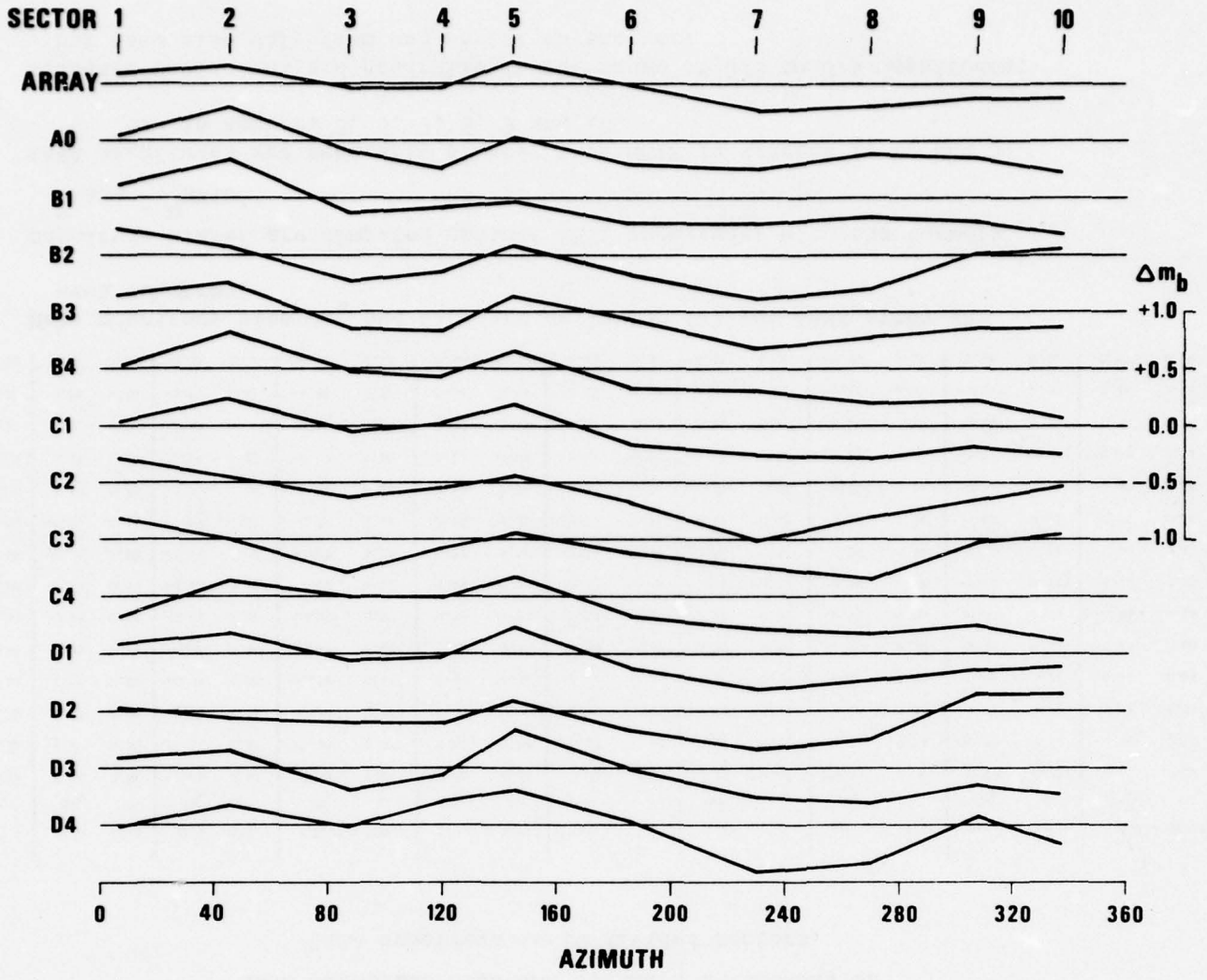

Figure 2. Azimuthal variations of LASA subarray magnitude bias. Δm_b of all subarrays follow general trends indicating such variations are the effects of the deeper structure which affects all subarrays.

TABLE IV

Mean magnitude bias and standard deviations of LASA subarrays in 10 divided sectors.

SECTOR	1		2		3		4		5		6		7		8		9		10		ALL
AZI	350.1 - 25.0		25.1 - 65.0		65.0 - 110.0		110.1 - 130.0		130.1 - 160.0		160.1 - 210.0		210.1 - 250.0		250.1 - 290.0		290.1 - 325.0		325.1 - 350.0		$\overline{\Delta m_b}$
	Δm_b	σ	Δm_b	σ	Δm_b	σ	Δm_b	σ	Δm_b	σ	Δm_b	σ	Δm_b	σ	Δm_b	σ	Δm_b	σ	Δm_b	σ	
LASA	0.07	0.29	0.14	0.41	-0.05	0.28	-0.05	0.20	0.18	0.32	-0.04	0.29	-0.25	0.42	-0.22	0.36	-0.13	0.35	-0.13	0.18	-0.05
A0	0.04	0.32	0.27	0.38	-0.11	0.35	-0.26	0.21	0.01	0.34	-0.24	0.28	-0.27	0.41	-0.12	0.34	-0.16	0.32	-0.28	0.10	-0.11
B1	0.11	0.29	0.33	0.34	-0.14	0.25	-0.09	0.17	-0.04	0.35	-0.24	0.33	-0.24	0.42	-0.18	0.39	-0.22	0.32	-0.32	0.22	-0.10
B2	0.21	0.33	0.05	0.39	-0.24	0.34	-0.18	0.15	0.06	0.31	-0.19	0.29	-0.40	0.39	-0.31	0.33	-0.00	0.32	0.02	0.14	-0.10
B3	0.14	0.30	0.24	0.35	-0.16	0.36	-0.19	0.21	0.11	0.33	-0.08	0.32	-0.33	0.42	-0.23	0.33	-0.15	0.32	-0.14	0.09	-0.08
B4	0.01	0.30	0.32	0.34	-0.02	0.32	-0.07	0.19	0.15	0.33	-0.17	0.29	-0.19	0.43	-0.30	0.38	-0.27	0.33	-0.44	0.18	-0.10
C1	0.02	0.29	0.23	0.32	-0.05	0.30	0.02	0.21	0.19	0.35	-0.17	0.38	-0.25	0.39	-0.28	0.39	-0.18	0.34	-0.25	0.23	-0.07
C2	0.21	0.25	0.04	0.43	-0.13	0.38	-0.04	0.23	0.07	0.35	-0.17	0.31	-0.50	0.37	-0.29	0.34	-0.15	0.31	-0.02	0.12	-0.10
C3	0.19	0.35	-0.00	0.36	-0.29	0.37	-0.07	0.21	0.06	0.31	-0.12	0.32	-0.23	0.41	-0.33	0.34	-0.02	0.33	-0.05	0.16	-0.08
C4	-0.18	0.29	0.15	0.38	-0.00	0.39	-0.01	0.20	0.18	0.31	-0.17	0.28	-0.27	0.41	-0.31	0.39	-0.25	0.33	-0.38	0.14	-0.12
D1	0.08	0.33	0.17	0.35	-0.07	0.25	-0.04	0.28	0.23	0.37	-0.13	0.33	-0.31	0.42	-0.23	0.38	-0.15	0.33	-0.13	0.22	-0.06
D2	0.02	0.33	-0.07	0.36	-0.11	0.30	-0.11	0.26	0.08	0.34	-0.17	0.24	-0.33	0.41	-0.25	0.35	-0.14	0.31	0.14	0.15	-0.09
D3	0.08	0.31	0.16	0.35	-0.19	0.42	-0.06	0.22	0.34	0.32	-0.01	0.28	-0.26	0.41	-0.32	0.32	-0.16	0.30	-0.25	0.19	-0.07
D4	-0.01	0.30	0.17	0.34	-0.02	0.24	0.20	0.21	0.30	0.31	0.03	0.26	-0.41	0.36	-0.34	0.33	0.06	0.34	-0.17	0.25	-0.02

Mean magnitude bias Δm_b and standard deviation (σ) for LASA array and each subarray.

Magnitude biases are computed against NEIS magnitudes with the formula $M_{LASA} - M_{NEIS}$.

LASA magnitudes are generally greater than NEIS in sectors 1, 2, and 5; but less in sectors 3, 6, 7, 8, 9 and 10.

Standard deviations are generally in the range of 0.3 to 0.4 magnitudes; but they also vary from one sector to another.

arrays, indicating that azimuthal variations of magnitude bias are acting uniformly over most subarrays, although some variations in each sector are either greater or less than the average magnitude bias.

If factors causing m_b bias in subarrays may be separated into regional and local structural changes, then the appearance of Δm_b variations acting uniformly in Figure 2 would show regional variation and the plot of Δm_b within each sector (Figure 3) would reflect local structural changes. Based upon this assumption, the regional cause is deeper than the local cause and, therefore, the regional cause may be the P-wave velocity and Q variations of the upper mantle (Evernden, 1977). Consider that LASA is located at the edge of the Western United States structure and that Q might be higher in the north and northeast of LASA and lower in the Southwest and West. Consequently, events at LASA from sectors 1 and 2 might show slightly positive magnitude bias and events in sectors 7 and 8 might show strongly negative bias as is observed. This is, of course, only proof of consistency, and other causes such as source regional NEIS bias, or source radiation pattern, are possible.

Contoured Patterns of Subarray Sector Magnitude Biases -- a Local Effect

Figure 3 shows contour maps of average magnitude bias by sector; the arrow in the figure shows direction of the incoming signal. Although small, these Δm_b contours show a close resemblance to similar contours made of travel-time anomalies (Iyer, 1971). The most conspicious pattern in the contour maps of Δm_b is the N60°E trend, which is in good agreement with the contoured travel-time anomalies presented by Aki et al., (1976), Iyer, (1971) and Greenfield and Sheppard (1969).

Interpretations of the N60°E trend of travel-time anomaly data is somewhat uncertain. Greenfield and Sheppard, as well as Iyer, suggested this trend indicated that the Moho boundary is sloping upward from under AO toward the southeast. However, Aki et al. (1967) and Capon (1974) suggested that perhaps such shallowing of the Moho is exaggerated. While we can offer no conclusive evidence, our interpretation of contour lines in Figure 3 is

---

Capon, J., 1974. Characterization of crust and upper mantle structure under LASA as a random medium, Bull. Seism. Soc. Am., 64, 235-266.

Figure 3. Contour maps of average m_b bias in 10 divided sectors. The variations in contour lines suggest the influence of variations in local crust upper-mantle structure (located at the end of the report as a foldout).

consistent with Greenfield's structure.

Figures 4a, 4b, and 4c, show NW-SE cross sections of LASA cutting from D4 to D2. The depth of the Moho was taken from the crustal structure in Figure 4 of Iyer's (1971) article. The 18° updip of the Moho boundary, beginning at A0 and moving toward the SE is in agreement with the model that Greenfield and Sheppard (1969) proposed, except that in their paper the Moho appears deeper than it was placed by Iyer. A simple velocity model of 6 km/sec for the crust and 8 km/sec for the mantle is used in this study to compute the incident wave refractions at the Moho boundary.

In Figure 4a, where seismic rays are emerging in parallel with the trend of the thinning crust under LASA, the rays are slightly convergent. The convergence appears between B2 and A0, which agrees with the contour lines in Figure 3 for Sectors 2 and 7. Note that this interpretation is based upon a simple model that previous workers suggested. Contour-line features appear to be simpler in the NW corner (on the flat crust side) and more complex toward the SE (thinning crust side).

Figure 4b shows the case corresponding to events in Sector 5, with the average angle of incidence of seismic waves of 25° (corresponds to events from Chile-Boliva border area); waves will be divergent at the surface because they will encounter the updip Moho structure. The divergent feature is rather simple in this case, the effect of the varying crustal thickness appears on the contour lines as the broadening of line spacing. This feature will begin as a N60° trend lying between D4 and B4 and continue toward the SE. Contour lines in Sectors 4 and 5 agree well with this explanation.

Figure 4c shows waves emerging from the NW corresponding to Sector 10 contour lines. An emergence angle of 16° was used which corresponded to events from the Tashkent area. The upgoing rays are convergent at the surface near B2. The waveforms are complex because converging rays and contour lines are narrowly spaced with a N60%E trend. Such features agree well with Sector 10 contour lines in Figure 3.

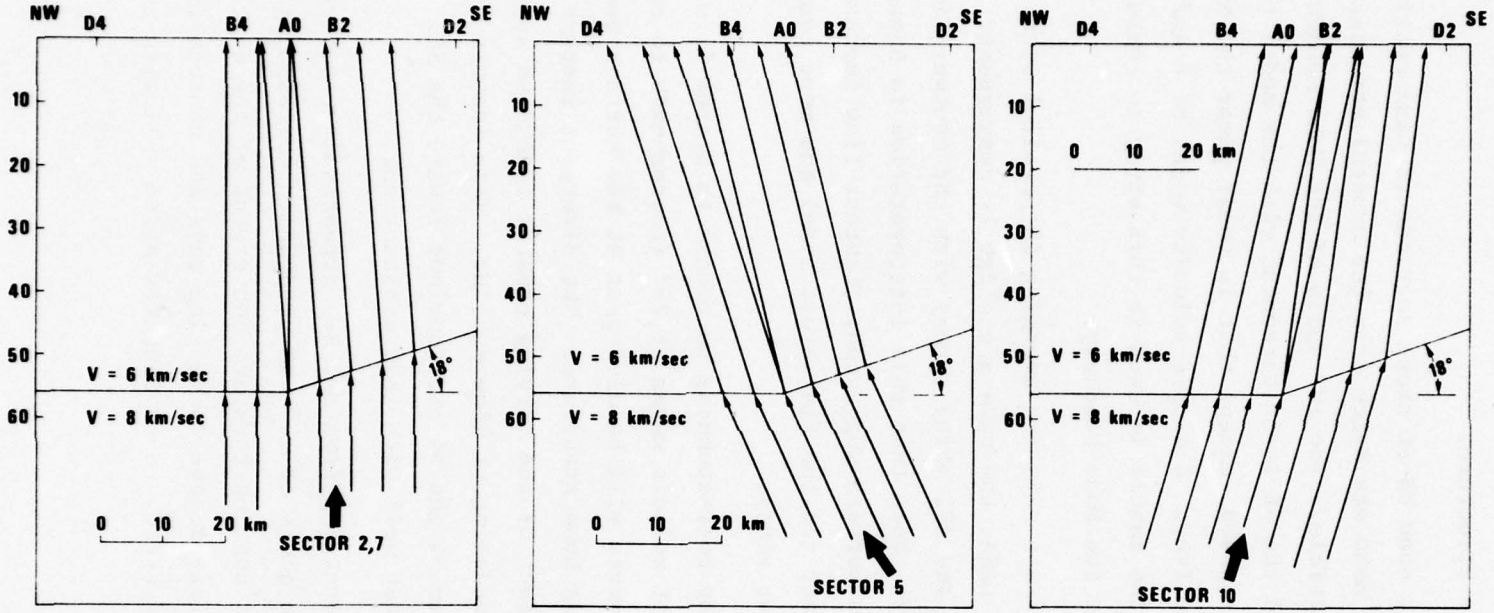

4a 4b 4c

Figure 4. Schematic paths for rays emergent at LASA subarrays with an uphill slope toward SE of the crustal boundary as suggested by Iyer. The effect of such structure gives a complicated appearance to the contour lines for events emerging from NW direction, and simpler feature for events from SE direction.

In addition to the NE-SW trend of these contour lines Figure 3 also shows some local, small-scale magnitude highs and lows. These small features may be the shadow of local heterogeneities such as small "bumps" in the Moho boundary or small local low Q zones. As the azimuth of emerging waves changes from one sector to another, these features show corresponding responses on the surface. Judging from the relative movements of these small feature against the NE-SW trend, small irregularities are likely to be located either directly above or below the Moho boundary.

To investigate the relation between amplitude and travel-time anomalies, some values of travel-time anomalies, Δt, were chosen from Chiburis' and Ahner's (1973) work. Selection was made based upon the location of events shown in Figure 1; then one location was chosen per sector where most events occurred in that sector. Although selecting one representative location in a sector was difficult, the choices may be adequate for first-order estimates of amplitude and travel-time anomaly relations. After determining a representative location, travel-time anomalies of that location where taken from the Chiburis-Ahner travel-time correction table. This method was simpler than the more precise method of relating travel-time corrections of each subarray, sector, and event, Δt_{ijk}, with Δm_{ijk}.

Figure 5 shows the plot of Δm_b against Δt for each sector, where Δm_b's are values shown in Table IV, and Δt's are Chiburis-Ahner correction values. Although some wide scattering exists, perhaps a result of selecting only one location per sector, amplitude and travel-time anomalies are linearly and clearly related; that is, positive Δm_b is related to positive Δt. Note that this is opposite to the relation discussed in Evernden's (1977) article, where he suggested that high attenuation (negative Δm_b) and positive (late) Δt correlated in the case of broad regional m_b anomalies. The linear relation in Figure 5 suggests that the LASA subarray effects, which are interpreted to be shallower than the regional effect, are generally consistent

---

Chiburis, E. F., and R. O. Ahner, 1973. LASA regional travel-time corrections and associated modes, SDAC-TR-73-6, Teledyne Geotech, Alexandria, Virginia, 22314.

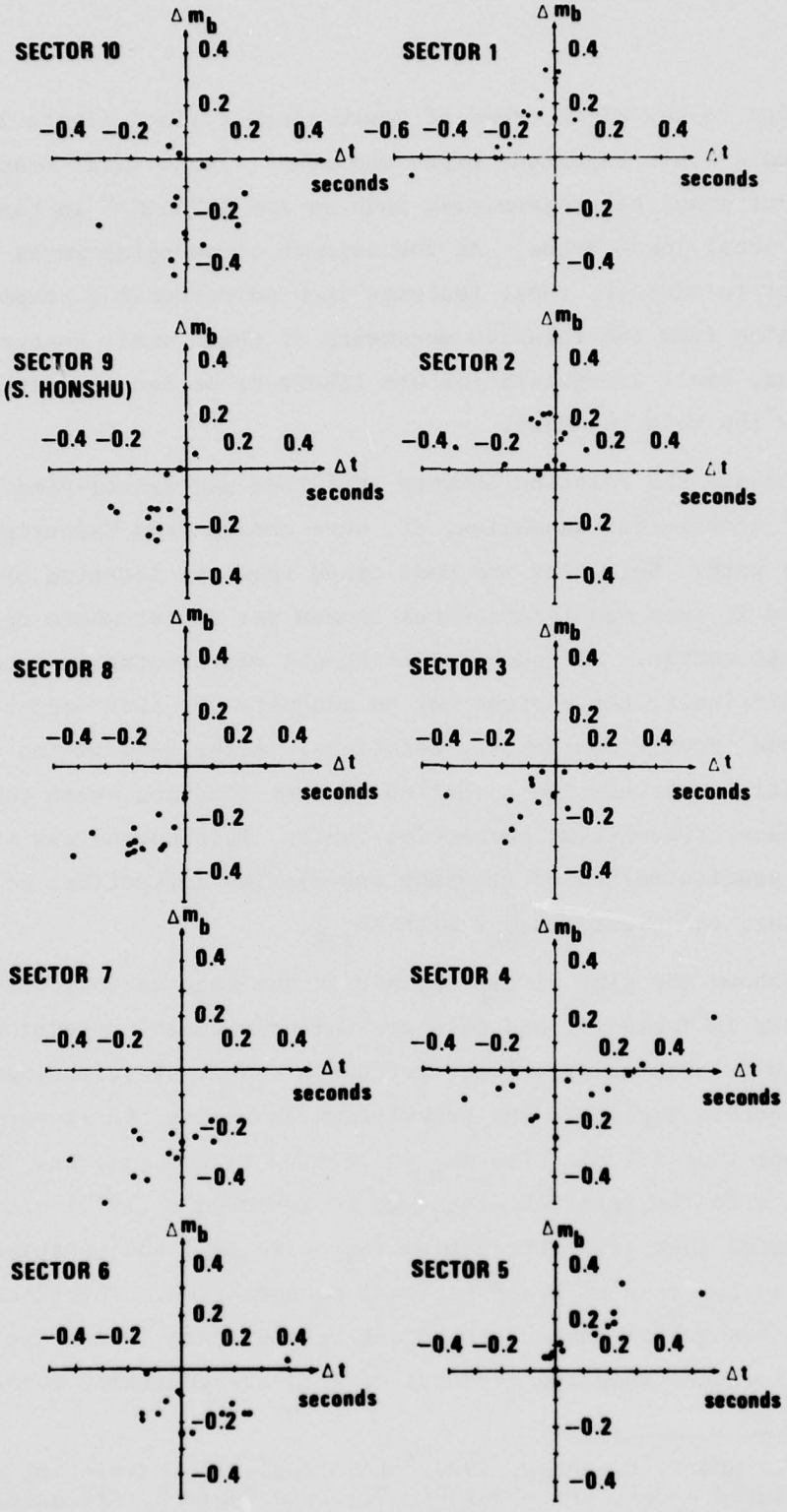

Figure 5. The relation of magnitude bias and travel-time anomalies at LASA subarrays in each sector.

with ray theory. For example, if a small body of high velocity, shaped as as a lens, exists in the upper mantle, then seismic rays through this lens will be divergent and the ray arrives earlier (negative Δt) than normal to the receiver above the lens and is associated with smaller (divergent) amplitude. Conversely, for low-velocity lens seismic rays will be convergent and ray arrives later (positive Δt) with positive Δm_b.

Because the low Q zone is deep, a negative Δm_b effect will be uniform for all subarrays. The net result is a shift of the coordinate origin downward (Since Δt are relative to A0 there is no effect on Δt.) In this context Figure 5 (and Figure 2) shows that Sectors 6, 7, and 8 are associated with coordinate shifts, and inspection of other sectors demonstrates that while Sector 1, 2, and 5 have positive coordinate shifts, Sectors 3 and 4 need no origin shift. This overall situation is consistent with the theory that a low Q zone exists in the WUS and that LASA is situated just at the edge of this zone, so that events in Sectors 1 and 2 seem to show the effect of waves travelling through Canadian-shield type mantle and events from the SW, W and NW (Sectors 6, 7, and 8) show the effects of waves travelling through the high attenuation zone of the WUS mantle.

In summary, a comparison of LASA and NEIS magnitudes suggests that all station magnitude biases should be calibrated azimuthally rather than with a single-value bias term. The data also shows that magnitude biases are affected by regional upper-mantle attenuations, as well as by local irregular structures located within the upper 100 km of the earth's crust, and that linear positive relation of amplitude and travel-time anomalies suggests that focussing due to local crustal irregularities is probably the main cause of magnitude anomalies within the array. Finally, it was revealed that a standard deviation of 0.3 m_b, with respect to NEIS, exists even after providing a good local and azimuthal correction; this is presumably due to earthquake radiation patterns and other source effects which "focus" a varying proportion of energy toward LASA.

FORMAL ANALYSIS OF VARIANCE FOR LASA MAGNITUDES

Thus far, simple models have been used to make inferences from LASA amplitudes or magnitudes concerning the bias of LASA relative to NEIS, the nature of the differences between the array beam and subarray beams, and structural effects causing scatter. A relatively large standard deviation, 0.15 m_b existed for magnitudes recorded over the 13 LASA subarrays studied. In this section, to describe this scatter and to estimate expected amplitude variation among nearby receivers, a more complex model will now be fit to this LASA data. The results can be applied to predictions of magnitude variation at a single station using closely-spaced sources.

Fixed Effects Model for LASA Magnitudes

Assume the following model to describe the LASA magnitude data:

$$m_{ijk}^{LASA} - m_{jk}^{NEIS} = \mu + \alpha_i + \gamma_{ij} + \beta_j + \delta_{jk} + e_{ijk} \qquad (9)$$

or

$$y_{ijk} = \mu + \alpha_i + \gamma_{ij} + \beta_j + \delta_{jk} + e_{ijk} \qquad (10)$$

where

m_{ijk}^{LASA} = magnitude measured at the i-th subarray for the k-th event in sector j,

m_{jk}^{NEIS} = magnitude reported by NEIS for the k-th event in sector j,

μ = mean LASA magnitude bias relative to NEIS magnitude for all events,

α_i = i-th subarray effect,

β_j = j-th sector (azimuth) effect,

γ_{ij} = interactions between i-th subarray and j-th sector,

δ_{jk} = k-th event effect within sector j,

e_{ijk} = a random, normally-distributed noise term with zero mean and variance σ_e^2.

This is a fixed-effect model with interactions; a detailed presentation of the model can be found in Scheffe (1959). Note that δ_{jk} terms are not interactions, but rather nested effects within each j-th sector.

Scheffe, H., 1959. The Analysis of Variance. New York, John Wiley and Sons, Inc.

Although equalizing the number of events from each sector was not necessary to arrive at an analytical solution for the various terms, we used only events in the data base recorded properly at all subarrays for each sector. To reduce the computations, the number of events in a sector was kept under fifty. This restriction resulted in no significant loss of precision in the estimated terms, and most sectors had initially fewer than fifty events (Appendix A). For each j-th sector, then, the k index runs from 1 to a variable k_j. To arrive at independent solutions for the terms, these essential side conditions were imposed:

$$\alpha_{\cdot} = \beta_{\cdot} = \delta_{j\cdot} = \gamma_{\cdot j} = \gamma_{i\cdot} = 0$$

where the dot notation means averaging over the index it replaces. With these conditions, the least-square estimates are obtained as

$$\begin{aligned}
\hat{\mu} &= y_{\cdots} \\
\hat{\alpha}_i &= y_{i\cdot\cdot} - y_{\cdots} \\
\hat{\beta}_j &= y_{\cdot j\cdot} - y_{\cdots} \\
\hat{\gamma}_{ij} &= y_{ij\cdot} - y_{i\cdot\cdot} - y_{\cdot j\cdot} + y_{\cdots} \\
\hat{\delta}_{jk} &= y_{\cdot jk} - y_{\cdot j\cdot}
\end{aligned}$$

The estimates for $\hat{\mu}$ and the $\hat{a}_i$'s, $\hat{\beta}_j$'s, and $\hat{\lambda}_{ij}$'s are listed in Table V. Based upon initial estimates of the above parameters in the model, the e_{ijk} term

$$\hat{e}_{ijk} = y_{ijk} - \hat{\mu} - \hat{\alpha}_i - \hat{\gamma}_{ij} - \hat{\beta}_j - \hat{\delta}_{jk} \qquad (11)$$

was used to identify large measurement errors in the data base. Although each observation with $|\hat{e}_{ijk}| > 0.3$ was rechecked, only a few readings were found in error, and these were eliminated or changed before computing final estimates of the model parameters.

According to Scheffe's (1959) work, an analysis-of-variance framework can be constructed for the particular model shown in Table VI. Tests for significance of the various terms in the model are in the form

$$\frac{SS_x/DF_x}{SS_e/(N_o - J(I-1) - N_q)} > F_{a,DF_x,N_o-J(I-1)-N_q}$$

TABLE V

Two-dimensional m_b bias estimation with a fixed-effect model.

$$m_{ijk}^{LASA} - m_{jk}^{NEIS} = \mu + \alpha_i + \beta_j + \gamma_{ij} + \delta_{jk} + e_{ijk}$$

No. of events = 222

No. observations = No. of events x 13 = 2886

Mean $\hat{\mu} = -0.09$

Station Effects	A0	B1	B2	B3	B4	C1	C2	C3	C4	D1	D2	D3	D4
$\alpha(i)$, i = 1, 13	-0.02	-0.02	-0.02	0.01	-0.01	0.01	-0.02	0.00	-0.03	0.03	-0.01	0.02	0.07

Sector Effects	1	2	3	4	5	6	7	8	9	10
$\beta(j)$, j = 1, 10	0.19	0.22	-0.05	0.03	0.26	-0.03	-0.21	-0.19	-0.15	-0.07

Interactions $\gamma(ij)$	A0	B1	B2	B3	B4	C1	C2	C3	C4	D1	D2	D3	D4
1	-0.01	0.06	0.16	0.06	-0.05	-0.06	0.13	0.12	-0.21	-0.02	-0.03	0.00	-0.15
2	0.14	0.20	-0.13	0.10	0.22	0.08	-0.14	-0.21	0.11	-0.05	-0.23	-0.03	-0.07
3	0.02	0.00	-0.09	-0.04	0.10	0.06	0.03	-0.17	0.14	0.02	0.03	-0.09	0.01
4	-0.17	0.00	-0.09	-0.13	0.01	0.07	0.05	-0.00	0.10	0.00	-0.02	-0.01	0.21
5	-0.08	-0.15	-0.06	-0.02	0.04	0.04	-0.04	-0.09	0.09	0.09	-0.08	0.17	0.11
6	-0.06	-0.08	-0.02	0.04	-0.02	-0.03	-0.02	0.02	-0.01	-0.02	-0.01	0.11	0.11
7	0.07	0.08	-0.08	-0.04	0.12	0.05	-0.17	0.07	0.08	-0.02	-0.01	0.03	-0.17
8	0.17	0.11	-0.02	0.03	-0.03	-0.02	-0.01	-0.07	-0.01	0.01	0.04	-0.05	-0.14
9	0.01	-0.07	0.14	-0.01	-0.14	-0.07	0.01	0.12	-0.09	-0.02	0.00	-0.03	0.15
10	-0.09	-0.14	0.21	0.02	-0.26	-0.10	0.17	0.21	-0.18	0.01	0.32	-0.10	-0.07

TABLE VI

Framework for the analysis of variance in the fixed-effects model for LASA magnitudes.

SOURCE OF VARIANCE	SUM OF SQUARES		DEGREES OF FREEDOM	
	Expression	Value	Expression	Value
α Effects	$SS_\alpha = N_q \sum_{i=1}^{I} (y_{i..} - y_{...})^2$	2.0	I-1	12
β Effects	$SS_\beta = I \sum_{j=1}^{J} K_j (y_{.j.} - y_{...})^2$	102.0	J-1	9
δ Effects	$SS_\delta = I \sum_{j=1}^{J} \sum_{k=1}^{K_j} (y_{.jk} - y_{.j.})^2$	255.0	N_q - J	212
γ Effects	$SS_\gamma = \sum_{i=1}^{I} \sum_{j=1}^{J} K_j (y_{ij.} - y_{i..} - y_{.j.} + y_{...})^2$	27.3	(I-1) (J-1)	108
Noise	$SS_e = \sum_{i=1}^{I} \sum_{j=1}^{J} \sum_{k=1}^{K_j} (y_{ijk} - y_{ij.} - y_{.jk} + y_{.j.})^2$	29.7	$N_o - J(I-1) - N_q$	2544
Total	$SS_t = \sum_{i=1}^{I} \sum_{j=1}^{J} \sum_{k=1}^{K_j} (y_{ijk} - y_{...})^2$	416.00	$N_o - 1$	2885

N_q - number of earthquakes (222)

N_o - number of observations (2886)

I - number of subarrays (13)

J - number of sectors (10)

where x stands for α, β, δ, or γ and DF_x for the degrees of freedom associated with parameter x. N_q and N_o are the number of earthquakes and observations, respectively, thus, $N_o = N_q \times 13$ subarrays. The F-statistic test was exceeded for each of the terms at the a = .99 level of confidence, making that model appropriate for LASA magnitudes. Contrasts among main effects α_i for the subarrays can be tested, an exercise showing that the α_i values for proximate subarrays may be closer in value, but not significantly different, than for those of more distant subarrays. Using Scheffe's T-method of comparison, contrasts among the subarray effects in the D, C, and even B rings were established to be, at a high confidence level, non-zero in most cases, even though the range in the α_i's is small. Even greater confidence exists for contrasts among sector effects β_j because of their larger range.

Event effects δ_{jk} were not listed in Table V, but they were generally large, ranging from nearly -1 to +1 magnitude unit. Assuming that NEIS magnitudes are unbiased estimates, interpretations of event effects δ_{jk} must, in terms of source radiation pattern and geophysical anomalies, be peculiar to the exact source-LASA path. Although subdividing the 10 sectors into more numerous event regions would reduce the scatter of these terms within a sector, this refinement was unwarranted because of an increase in degrees of freedom.

The μ term at LASA has an overall -0.09 magnitude bias for seismic events within 100° around the globe, a figure in good agreement with this study's earlier analysis. The α_i term represents the mean bias of subarray magnitudes relative to μ. Their small range implies that a gross station effect (or correction term) will vary only slightly over the dimension of LASA, roughly 50 km, and that station effects are not the cause of the large magnitude scatter at LASA. The larger β_j effects are azimuthally-dependent gross correction terms due to the structure in the crust and upper mantle under LASA. However, a portion of these effects can be attributed to consistent source or path bias relative to LASA for events within the delineated sectors. For example, Sector 7 is dominated by earthquakes in the Fiji-Tonga-Kermadec region, where the fault-plane strikes have fairly consistent azimuths relative to LASA.

The interactions γ_{ij} in Table V are random and have a range of nearly 0.5 m_b unit. These terms are closely related to the effects on signal wave

forms from the laterally inhomogenous structure beneath LASA and they absorb much of the scatter represented by the high values resulting when equation (8) was applied.

The noise term in our model, e_{ijk}, is statistically represented by its estimated variance, computed as .011 using the form in Table V; thus σ = 0.104. Assuming a normal distribution for the noise term implies that for 5% of the observations the error exceeds an absolute value of 0.21 m_b unit. Thus, even a detailed model does not adequately represent observed magnitude at a LASA subarray, if a confidence factor of two in the predicted value is required. Further, this result ignores the large and capricious values of the δ_{jk}'s, which are mostly unpredictable and add as much as ±1.0 to the uncertainty in absolute source magnitude.

Nature of Station Magnitude Corrections

Several investigators have already obtained seismic station magnitude corrections independent of azimuth (Cleary, 1967; Carpenter et al., 1967; Evernden and Clark, 1970; Booth et al., 1975; North, 1977). The results presented here for LASA provide some gauge of the utility of such corrections when applied to any given event. Consider each LASA subarray as a distinct station with a correction given by

$$\hat{C}_{ij} = \hat{\mu} + \hat{\alpha}_i + \hat{\gamma}_{ij} + \hat{\beta}_j. \qquad (12)$$

This definition includes the sector effect and its interaction with each subarray and it is a more precise station correction than a gross single-dimension station term. Although subdividing the sectors into small source regions,

---

Cleary, J., 1976. Analysis of the amplitude of short-period P-waves recorded by Long Range Seismic Measurements stations in the distance range 30 to 102 degrees, J. Geophys. Res., 72, 4705-4712.

Carpenter, E. W., P. D. Marshall, and A. Douglas, 1967. The amplitude-distance curve for short-period teleseismic P-waves, Geophys. J. R. Astr. Soc., 13, 61-70.

Evernden, J. F., and D. M. Clark, 1970. Study of teleseismic P. II-Amplitude data, Phys. E. Planet. Int., 4, 24-34.

as Berteussen and Husebye (1974) did with NORSAR amplitude, can achieve further precision, the present limited data base will not allow such refinement for most sectors. Recall that the main effects α_i and β_j, and their interactions, were found, at very high confidence levels, to be significantly different from zero. Thus, plots of C_{ij} in Figure 6 for all the subarrays can be presented as meaningful data. In each case, connected sector points have a positive or negative residual relative to the NEIS reference set represented by the dashed circle, with radius equal to one magnitude unit, and an angle equivalent to the center azimuth of each sector. In this figure important phenomena represented include the large azimuthal variations at any given subarray and the imperfect correlation of patterns among the subarrays that span an area roughly 50 km in diameter. Evidently, "station correction" is a highly variable quantity.

If from equation (9) a prediction of event magnitude from a single observation is given by

$$\hat{m}^{NEIS}_{ij}(i) = m^{LASA}_{ijk} - \hat{\mu} - \hat{\alpha}_i - \hat{\gamma}_{ij} - \hat{\beta}_j, \tag{13}$$

then the difference between prediction and actual observation is

$$m^{NEIS}_{jk} - m^{NEIS}_{jk}(i) \approx \hat{\delta}_{jk} + e_{ijk} \tag{14}$$

Note that δ_{jk} cannot be known a priori and, therefore, cannot be used to correct station magnitudes before a mean event magnitude is estimated from many stations. From this analysis of LASA magnitudes, $\hat{\delta}_{jk}$ has a range of roughly two magnitude units and, e_{ijk}, with a standard deviation of approximately 0.1, is negligible in comparison. Thus, $\hat{C}_{ij}$, which Figure 6 shows has a spread of less than one magnitude unit, accounts for no more than one-half the observed magnitude difference between a LASA subarray prediction and the NEIS magnitude. This result implies that, although using azimuthally-varying corrections can produce significant gains in precision of a stations's magnitude estimation, a significant portion of unpredictable error will still exist unless more detailed or regionalized corrections are developed.

Berteussen, K. A., and E. S. Husebye, 1974. Amplitude pattern effects on NORSAR P-wave detectability, NORSAR Scientific Report No. 1-74/75, Kjeller, NORWAY.

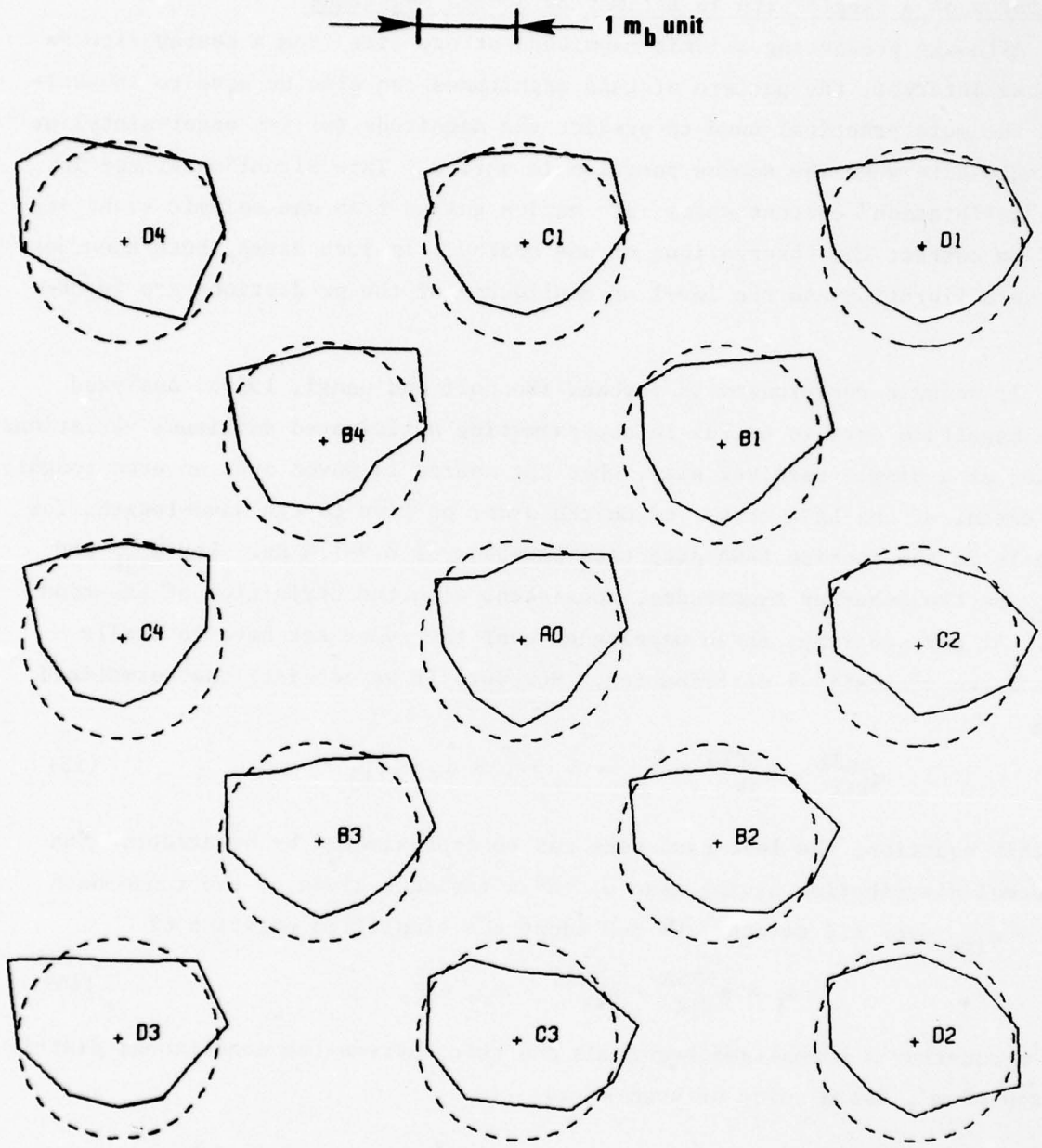

Figure 6. Azimuthal variations of LASA subarray magnitude corrections. Dashed circle in each subarray represents zero m_b correction. Inside the circle smaller subarray m_b is represented; thus, positive corrections should be applied, and vice-versa for points outside.

Precision of a Single Site in Estimating Source Magnitude

Although predicting seismic magnitude at one site from a nearby site is of some interest, the pattern of LASA magnitudes can also be used to investigate the more practical need to predict the magnitude (or its uncertainty) at a single site when the source position is varied. This situation arises in any "calibration" context where information gained from one seismic event is used to correct the observations of one nearby. In such cases, both accuracy of the calibration and the level of confidence of the predictions are important.

If seismic reciprocity is invoked (Knopoff and Gangi, 1959), analyzed LASA magnitude data is useful in approximating anticipated amplitude variations either at a single receiver site, when the source is moved over an area roughly the extent of the LASA array, or on the order of five to ten wave-lengths for signals in the routine LASA detection passband of 0.9-1.4 Hz. Let m_{ijk} and m'_{ijk} be two subarray magnitudes, consistent with the definition of equation (9). At any subarray, these magnitudes over the event set have no easily formulated statistical distribution. However, if we consider the normalized form

$$m_{ijk}^{LASA} - m_{jk}^{NEIS} - \hat{\delta}_{jk} - \hat{\beta}_j - \hat{\mu} = \hat{\alpha}_i + \hat{\gamma}_{ij} + e_{ijk} \qquad (15)$$

by this equation, the left-hand side can be approximated by a variable with a normal distribution having mean α_i and a variance given by the randomness $\gamma_{ij} + e_{ijk}$ over all events. We now adopt the simplified notation of

$$m_i = m_{ijk}^{LASA} - m_{jk}^{NEIS} - \hat{\delta}_{jk} - \hat{\beta}_j - \hat{\mu} \qquad (16)$$

for a subarray's normalized magnitude and then express the conditional distribution of m', for a suite of events, as

$$f(m_{i'}|m_i) = \frac{1}{\sqrt{2\pi}\ \sigma_{i'}\ \sqrt{1-\rho_{ii'}^2}}\ \exp\left[-\frac{(m_{i'} - \phi_{ii'})^2}{2(1-\rho_{ii'}^2)\ \sigma_{i'}^2}\right] \qquad (17)$$

Knopoff, L., and A. F. Gangi, 1959. Seismic Reciprocity Geophysics, 24 (4) 681-691.

where the mean $\phi_{ii'}$ is given by

$$\phi_{ii'} = \rho_{ii'} \frac{\sigma_i}{\sigma_{i'}} (m_i - \alpha_i) + \alpha_{i'} \tag{18}$$

Equation (17) is the relation appropriate to jointly-distributed, normal, correlated variables. To determine $\rho_{ii'}$, we compute the covariance of m_i and $m_{i'}$

$$\sigma^2_{ii'} = \frac{1}{J} \sum_j \frac{1}{K_j} \sum_k (m^{LASA}_{ijk} - m^{NEIS}_{jk} - \hat{\delta}_{jk} - \hat{\beta}_j - \hat{\mu} - m_{i..}) \cdot$$
$$(m^{LASA}_{i'jk} - m^{NEIS}_{jk} - \hat{\delta}_{jk} - \beta_j - \hat{\mu} - m_{i'..}) \tag{19}$$

and the variance of m_i as

$$\sigma^2_i = \frac{1}{J} \sum_j \frac{1}{K_j} \sum_k (m^{LASA}_{ijk} - m^{NEIS}_{jk} - \hat{\delta}_{jk} - \hat{\beta}_j - \hat{\mu} - m_{i..})^2 \tag{20}$$

and similarly for $\sigma_{i'}{}^2$. The squared correlation coefficient is defined as

$$\rho^2_{ii'} = \frac{(\sigma_{ii'}{}^2)^2}{\sigma_i{}^2 \, \sigma_{i'}{}^2} . \tag{21}$$

Aki (1973) has already shown that $\rho_{ii'}$ is dependent upon the subarray spacing at LASA for spectral amplitudes near 1 Hz, a finding consistent with Chernov's (1960) theory. Figure 7 shows the $\rho_{ii'}$ computed for the 13 subarrays of this study. The trend is toward lesser correlation with increasing separation, which is similar to Aki's results because magnitudes measured in this study were associated with periods predominantly near one second. The $\sigma_i\sqrt{1-\rho_{ii}{}^2}$, values are also plotted which are the standard deviation of the conditional distribution of magnitude at one subarray, given that at another. These values are in part reflections of results displayed in Figure 6 on the amplitude patterns of the LASA subarrays.

How the principle of seismic reciprocity between sources and receivers (Knopoff and Gangi, 1959) is related to equality of amplitude variances is discussed in Appendix B. If reciprocity holds, then the correlations and uncertainties expressed in Figure 7 can be converted into appropriate uncertainties for an array of sources rather than receivers. For a pair of identical sources within ten km of each other, roughly the smallest inter-subarray

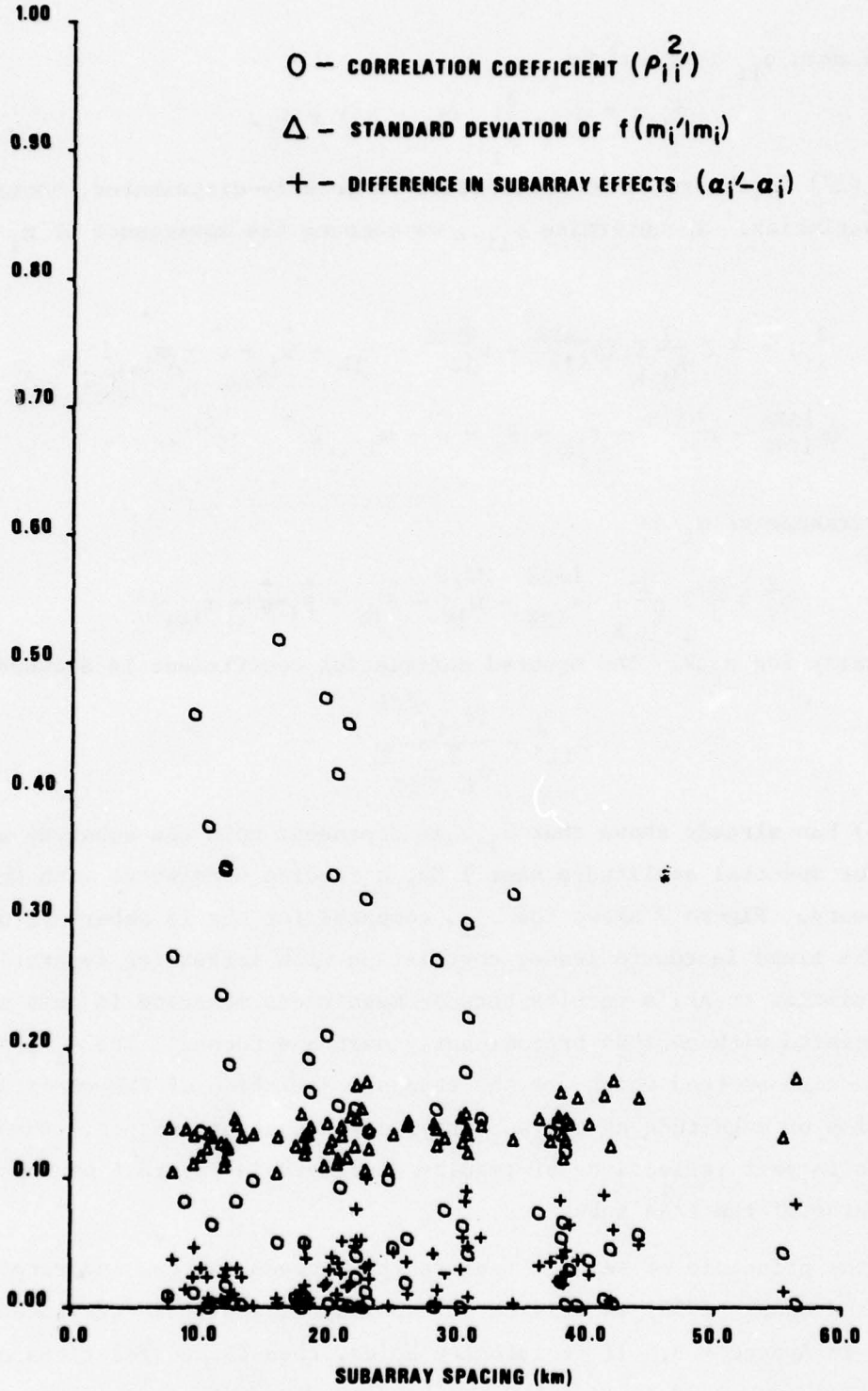

Figure 7. Estimates of signal amplitude correlations, variances, and differences versus receiver separation using LASA subarrays. By seismic reciprocity, this is an estimate of variations to be expected at a single site due to similar changes in source position.

distance at LASA (between A0 and B ring), correlation of the amplitudes received at a single fixed site should be near 0.5. Corresponding to this correlation the standard deviation of the measured magnitude for the second source minus that of the first source should be near 0.10. For maximum separation of sources corresponding to the LASA D-ring spacing, the correlation falls to around zero, and the standard deviation of the measured magnitude of the second source, relative to that of the first one, would be near 0.15. Note that the variation in the α_i is not considered here because it incorporates the specific peculiarity of the LASA structure and it cannot be projected into a statistical consideration of source regions. Its values (see Table V) were small at LASA and including it would add no more than 0.1 to the uncertainty for the largest separations and much less for the smallest separations considered.

These results imply that magnitude calibration for sources has a very limited range, probably less than is commonly thought satisfactory for a calibration of travel-time residuals, except in dipping-plate source regions. If LASA structure is similar to the crust and upper mantle in earthquake source regions, in terms of expected variations in magnitude, then a magnitude calibration for a given source-receiver pair cannot be expected to remain within 0.3 m_b unit with better than 95% confidence when a new source occurs just 50 km from the calibration source. Clearly, an advantage exists in multiple receivers because the improvement through network calibration should behave as the square root of the number of receivers.

The question of whether the conditions for seismic reciprocity are valid for the LASA array of receivers is not studied in this report. If, as Balachandran (1974) suggests for a smaller-scale experiment, the LASA seismometers are within a few wavelengths of the inhomogeneities that give rise to the amplitude and phase fluctuations found in this and numerous other studies, then reciprocity may not hold. The scatter of amplitudes, enhanced by secondary wave fields, over the LASA array may give too large an estimate of the scatter to be expected in the reciprocal case of an array of sources.

Balachandran, K., 1974. Noninterchangeability of sources and receivers in a heterogeneous medium, Geophysics, 39, 73-80.

BEHAVIOR OF LASA AMPLITUDES AS A FUNCTION OF SENSOR AND SOURCE SEPARATION

This section focusses on variations in receiver amplitudes as a function of increasing source separation. The discussion clarifies nearly all the important results of this report that pertain to statistical fluctuations of LASA amplitudes.

Consider the log amplitudes a_{ik} at two subarrays i and i′ for events k and k′, with k indexing over all events and not just those in a particular sector. Then the quantity

$$\Delta a = (a_{ik} - a_{i'k}) - (a_{ik'} - a_{i'k'})$$

measures the imprecision of the calibration of the subarray differences from one event to another. As already discussed, this quantity should be an increasing function of subarray separation and of event separation. Here we compute the standard deviation of Δa versus increases in both these separations thus,

$$\sigma[\Delta a(|\vec{r}|, d\gamma)] = \left[\frac{\sum_{N} [a_{ik} - a_{i'k}) - (a_{ik'} - a_{i'k'})]^2}{N-1} \right]^{\frac{1}{2}} \qquad (22)$$

where the summations is made over all subarray-event combinations falling within given incremental values of subarray separation $|\vec{r}|$ and central angle separation $d\gamma$. The $d\gamma$ is calculated as

$$d\gamma = \arccos (X_k X_{k'} + Y_k Y_{k'} + Z_k Z_{k'})$$

where

$$X_k = \sin i_k \cdot \cos \Theta_k$$
$$Y_k = \sin i_k \cdot \sin \Theta_k$$
$$Z_k = \cos i_k$$

and similarly for event k′. The angles i_k and Θ_k are the incidence angle and back azimuth of the signal arriving at LASA from event k. So $d\gamma$ is a measure of the central angle between the two rays that impinge on an imaginary hemisphere surrounding LASA. The epicentral distance and depth of the events, listed in Appendix I, are converted to an incidence angle by linear interpolation of the tables in Pho and Behe (1972).

When computing standard deviations according to equation (22), subarray separations were pooled in 10 km steps and $d\gamma$ pooled into bins of $< 1°$, $< 2°$, $< 4°$, etc. The truncated data base defined in the previous section was used as a means to avoid biasing the results with large concentrations of data from a few highly seismic areas. The epicenters were further limited to $\Delta > 30°$ from LASA because the $\underline{i}$ vs. Δ relation is highly dependent upon crustal-upper mantle structure at short distances. Also, epicenters with $\Delta < 90°$ were discarded because highly variable fluctuations were associated with even close epicenters because of core diffraction and plate effects on many of the events in this range from LASA (see Figure 1). With the 167 remaining events, $\sigma(\Delta a)$'s shown in Figure 8 were computed. Each point represen s no fewer than N=500 combinations summed in equation (22). The pattern here is relatively smooth, increasing from roughly $\sigma = .10$ for small $|\vec{r}|$ and small $d\gamma$ (in general agreement with results in previous sections) to nearly $\sigma = .40$ for the largest values of both. Therefore, results, shown in Figure 8 suggest that magnitude calibration is not precise for neighboring events and that it becomes almost meaningless for events distant from one another. Note that a given $d\gamma$ maps into values of inter-event distance which are dependent upon the relation of the event locations to the great-circle path back to the receiver. For example at $\Delta = 90°$, a 1° difference in $d\gamma$ translates to a 1° (~ 110 km) difference in epicenters perpendicular to the path but to roughly a 10° (~ 1100 km) difference in epicenters parallel to the path. Thus, magnitude calibration could be applicable to much larger source location changes if they are along the raypath direction rather than normal to it. However, calculations needed to precisely verify this principle were not performed.

Results similar to those for LASA in Figure 8 have been obtained for NORSAR using the data in Berteussen and Husebye (1974), but they are not presented here.

Pho, T.-T., and L. Behe, 1972. Extended distances and angles of incidence of P-waves, Bull. Seism. Soc. Am., 62, 885-902.

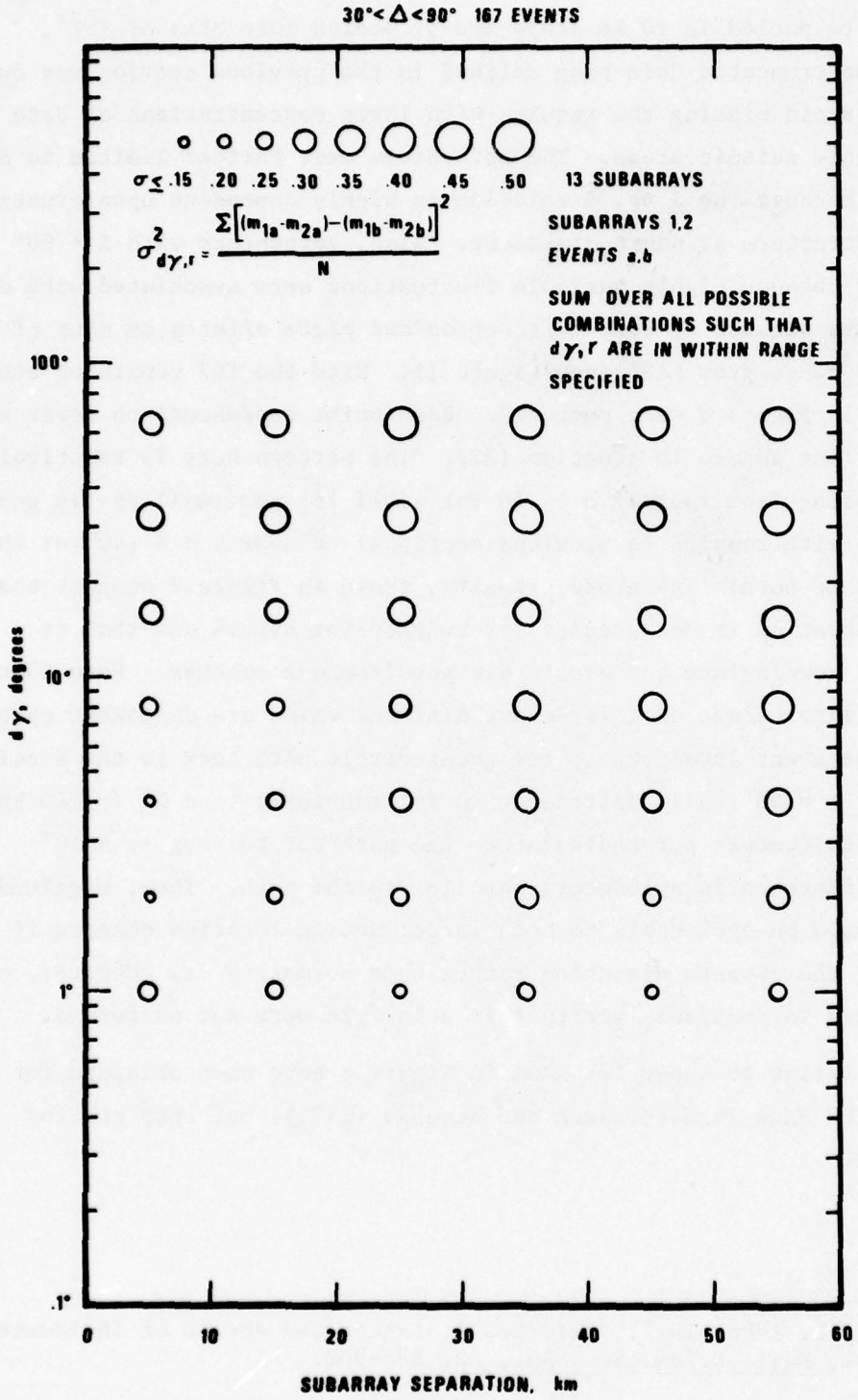

Figure 8. *Standard deviation of the imprecision of calibration,* $\sigma(\Delta m_b)$, *expressed in terms of subarray separation and the central angle between two rays impinging at LASA.*

CONCLUSION

LASA magnitude bias relative to NEIS, when averaged in all directions for the whole array, as well as individual subarrays, is near -0.1 m_b. However, when viewed in azimuthal sectors, LASA m_b biases reveal large coherent variations, indicating that generally accepted, single-value, station bias terms cannot reduce bias to negligible proportions for single stations magnitude observations, even if they are determined to be statistically significant with a large data base. Subarray azimuthal biases show uniform variation among subarrays, suggesting that the effect of regional bias, possibly related to upper-mantle attenuation, indeed exists at LASA. Interpretations of regional bias suggests that LASA is located at the edge of the anomalous Western United States structure. However, local crustal and upper-mantle heterogeneity apparently has an even greater effect than regional structure on the m_b bias of each subarray. The result is that local m_b biases also reveal characteristic features of crustal and upper-mantle structure and they show some linear correlation with values of travel-time residuals.

From the linear regression analysis standard deviations of subarray magnitudes were found to be at the 0.15 m_b level within each sector. Using the fixed effects model, these equivalent values are represented in the sector-subarray interaction term γ_{ij}, which also showed a similar range of fluctuations. Further, the event effect term δ_{jk} gives as much as much as 1.0 m_b uncertainty in source magnitude. Subarray effects were small when averaged over all events, and so they are not the cause of the large LASA magnitude scatter.

Within the context of station calibration, the confidence level of predicting the m_b at a station for an event from calibrations based on another event occurring in a nearby source area was examined. Assuming seismic reciprocity results showed that the correlation of a single receiver's magnitudes for repeated observations of two events occurring only 50 km apart from each other would be near zero. This result implies that magnitude calibration for sources is very limited in space, probably to an area much less than that believed to hold for the calibration of travel-time anomalies. Uncertainty is a factor of two (± 0.3 m_b), at the 95% confidence level, in predicted

amplitude at a station for a source moved only 50 km from the calibration source in a geologic area of complexity similar to LASA's. For sources several tens of degrees apart the magnitude uncertainty at the 95% confidence level is ± 0.8 m_b for stations 50 km apart in regions similar to LASA. To the extent that the crustal effects discussed in this report may be regarded as "random" in a network of stations, they may be miminized by network averaging.

ACKNOWLEDGEMENT

We acknowledge the assistance of D. P. J. Racine, M. F. Tillman, B. W. Barker, and W. Silverman in the amplitude and period analysis of LASA events. Drs. R. R. Blandford and Zoltan A. Der reviewed the typescript and made many suggestions for its improvement.

REFERENCES

Aki, K., 1973. Scattering of P-waves under the Montana LASA, J. Geophys Res., 78, 1334-1346.

Aki, K., A. Christofferson, and E. S. Husebye, 1976. Three dimensional seismic structure of the lithosphere under Montana LASA, Bull. Seism. Soc. Am., 66, 501-524.

Balachandran, K., 1974. Noninterchangeability of sources and receivers in a heterogeneous medium, Geophysics, 39, 73-80.

Berteussen, K. A., and E. S. Husebye, 1974. Amplitude pattern effects on NORSAR P-wave detectability, NORSAR Scientific Report No. 1-74/75, Kjeller, Norway.

Booth, D. C., P. D. Marshall, and J. B. Young, 1975. Long and short period amplitudes from earthquakes in the range 0° - 114°, Geophys. J. R. Astr. Soc., 39, 523-538.

Capon, J., 1974. characterization of crust and upper mantle structure under LASA as a random medium, Bull. Seism. Soc. Am., 64, 235-266.

Carpenter, E. W., P. D. Marshall, and A. Douglas, 1967. The amplitude-distance curve for short-period teleseismic P-waves, Geophys. J. R. Astr. Soc., 13, 61-70.

Chernov, L. A., 1960. Wave Propagation in a Random Medium. McGraw Hill, New York.

Chiburis, E. F., and R. O. Ahner, 1973. LASA regional travel-time correcitons and associated nodes, SDAC-TR-73-6, Teledyne Geotech, Alexandria, Virginia, 22314. AD 774458

Chiburis, E. F., and R. A. Hartenbeger, 1966. LASA signal and noise amplitudes for three teleseismic events, SDL Reprot No. 151, Teledyne Geotech, Alexandria, Virginia, 22314. AD 485 032L

Cleary, J., 1967. Analysis of the amplitude of short-period P-waves recorded by Long Range Seismic Measurement stations in the distance range 30 to 102 degrees, J. Geophys. Res., 72, 4705-4712.

Der, Z. A., 1976. On the existence, magnitude and causes of broad regional variations in body-wave amplitudes, SDAC-TR-76-8, Teledyne Geotech, Alexandria, Virginia, 22314.

Evernden, J. F., 1977. Regional bias in magnitude versus yield measurements: Its explanation and modes of evaluation. Submitted for publication.

Evernden, J. F., and D. M. Clark, 1970. Study of teleseismic P. II: Amplitude data Phys. E. Planet. Int., 4, 24-34.

Greenfield, R. J., and R. M. Sheppard, 1969. The Moho depth variations under LASA and their effect on dT/dΔ measurements, Bull. Seism. Soc. Am., 59, 409-420.

Husebye, E. S., A. Dahle, and K. A. Berteussen, 1974. Bias anslysis of NORSAR- and ISC- reported seismic event m_b magnitudes, J. Geophys. Res., 79, 2967-2978.

Iyer, H. M., 1971. Variation of apparent velocity of teleseismic P-waves across the Large-Aperture Seismic Array, Montana, J. Geophys. Res., 76, 8554-8567.

Klappenberger, F. A., 1967a. Distribution of short-period P-wave amplitude over LASA, SDL Report No. 187, Teledyne Geotech, Alexandria, Virginia, 22314. AD 815580

Klappenberger, F. A., 1967b. Spatial correlation of amplitude anomalies. SDL Report No. 195, Teledyne Geotech, Alexandria, Va. 22314. AD 819938.

Knopoff, L., and A. F. Gangi, 1959. Seismic reciprocity, Geophysics, 24, 681-691.

Lambert, D. G., D. H. von Seggern, S. S. Alexander, and G. A. Galat, 1969. The LONG SHOT experiment, Vol. 1: Basic observations and measurements, SDL Report No. 234, Teledyne Geotech, Alexandria, Virginia, 22314. AD 698 319

North, R. G., 1977. Station-magnitude bias-its determination, causes, and effects, Lincoln Laboratory, Technical Note 1977-24, Lexington, Massachusetts.

Pho, T.-T., and L. Behe, 1972. Extended distances and angles of incidence of P-waves, Bull. Seism. Soc. Am., 62, 885-902.

Scheffe, H., 1959. The Analysis of Variance. New York, John Wiley & Sons, Inc.

Veith, K. F., and G. E. Clawson, 1972. Magnitude from short-period data, Bull. Seism. Soc. Am., 62, 435-452.

APPENDIX A

List of events and event parameters used
in this study, grouped in sectors L01 to L10.

THIS PAGE IS BEST QUALITY PRACTICABLE
FROM COPY FURNISHED TO DDC

LASA MAGNITUDE, DMB=MLASA-MNEIS,SECTOR L01

35 EVENTS ARE ANALYZED FROM 350.1 TO 25.0 AZI

EPX NO.	DATE	MNEIS	MLASA	ML-MN	DIST	AZI	DEPTH	BFACTOR
11680	740404	5.10	4.98	-0.12	94.1	1.0	21.0	3.80
17290	740406	5.20	5.44	0.24	96.2	1.0	84.0	4.00
44000	740122	5.00	5.20	0.20	93.2	1.0	50.0	3.80
71495	740219	5.00	4.70	-0.30	97.3	2.0	85.0	4.00
72525	740220	5.10	5.44	0.34	92.6	0.1	25.0	3.90
46930	740426	5.00	4.58	-0.42	97.3	2.0	80.0	4.00
73035	740513	5.50	5.65	0.15	96.8	2.0	208.0	3.80
80906	740517	5.30	5.64	0.34	96.8	2.0	208.0	3.80
4180	740603	5.30	5.76	0.46	96.4	1.0	100.0	4.00
4590	740603	5.00	5.10	0.10	94.1	1.0	60.0	3.90
8785	740606	5.30	5.43	0.13	96.9	2.0	214.0	3.80
55675	740705	5.10	5.09	-0.01	95.9	1.0	33.0	4.00
81815	740723	5.00	4.89	-0.11	94.1	1.0	33.0	3.80
94396	740730	5.30	4.51	-0.79	97.7	1.0	70.0	4.00
4180	740804	5.40	6.03	0.63	87.6	20.0	33.0	3.80
11270	740808	5.20	5.19	-0.01	51.6	19.0	33.0	3.40
16505	740811	5.00	5.17	0.17	93.9	0.1	33.0	3.80
52430	740829	5.00	4.99	-0.01	96.7	1.0	228.0	3.90
53905	740829	5.20	5.15	-0.05	65.7	4.0	0.0	3.70
13815	741003	5.00	4.93	-0.07	96.8	2.0	198.0	3.80
3885	741113	5.10	5.02	-0.08	87.4	19.0	42.0	3.70
12305	741117	5.20	5.48	0.28	98.7	15.0	43.0	4.20
28345	741127	5.00	5.47	0.47	94.2	22.0	50.0	3.85
87460	741230	5.30	5.12	-0.18	97.2	3.0	116.0	4.00
51926	740130	5.40	5.78	0.38	83.4	357.0	0.0	3.70
61440	740710	5.30	5.39	0.09	83.4	357.0	0.0	3.70
17285	740811	5.10	5.14	0.04	94.0	359.0	12.0	3.80
17475	740811	5.10	4.91	-0.19	94.1	359.0	29.0	3.80
20170	740812	5.20	4.79	-0.41	94.1	359.0	27.0	3.80
50300	740827	5.30	5.40	0.10	93.9	359.0	33.0	3.80
77165	740912	5.20	5.13	-0.07	94.1	359.0	33.0	3.80
79285	740913	5.20	5.40	0.20	83.4	357.0	0.0	3.70
7765	740929	5.40	5.97	0.57	92.8	356.0	33.0	3.90
42750	741016	5.50	5.76	0.26	83.2	356.0	0.0	3.70
86595	741103	5.20	5.39	0.19	89.4	354.0	33.0	3.70

THIS PAGE IS BEST QUALITY PRACTICABLE
FROM COPY FURNISHED TO DDC.

LASA MAGNITUDE, DMB=MLASA-MNEIS,SECTOR L02

22 EVENTS ARE ANALYZED FROM 25.1 TO 65.0 AZI

EPX NO.	DATE	MNEIS	MLASA	ML-MN	DIST	AZI	DEPTH	BFACTOR
85505	741229	5.20	5.06	-0.14	48.4	35.0	33.0	3.60
64980	741214	5.00	4.48	-0.52	82.3	39.0	11.0	3.60
63290	741214	5.30	5.96	0.66	82.7	39.0	33.0	3.70
10705	741116	5.00	5.32	0.32	46.2	53.0	33.0	3.50
6380	741114	5.00	5.11	0.11	83.5	37.0	24.0	3.70
6350	741114	5.10	5.22	0.12	83.5	37.0	3.0	3.70
6305	741114	5.00	5.05	0.05	83.5	37.0	19.0	3.70
75625	741029	5.10	5.70	0.60	76.5	37.0	33.0	3.60
42541	741016	5.00	5.27	0.27	46.1	53.0	33.0	3.50
86205	740917	5.20	4.38	-0.82	81.0	38.0	17.0	3.50
64390	740904	5.10	5.34	0.24	83.6	46.0	17.0	3.70
73180	740717	5.10	5.78	0.68	78.7	31.0	145.0	3.60
60195	740709	5.00	4.79	-0.21	87.3	34.0	69.0	3.70
47835	740628	5.00	5.41	0.41	76.6	50.0	33.0	3.60
44760	740625	5.10	5.09	-0.01	48.3	35.0	33.0	3.60
39165	740622	5.10	5.41	0.31	81.2	36.0	36.0	3.50
33550	740620	5.10	4.76	-0.34	76.4	37.0	33.0	3.60
17770	740612	5.50	6.13	0.63	46.9	35.0	13.0	3.60
81016	740517	5.00	5.60	0.60	46.9	35.0	33.0	3.60
98820	740323	5.00	4.93	-0.07	43.9	53.0	33.0	3.20
98340	740322	5.00	4.80	-0.20	47.1	26.0	22.0	3.60
53670	740201	5.20	5.66	0.46	85.1	34.0	29.0	3.70

THIS PAGE IS BEST QUALITY PRACTICABLE
FROM COPY FURNISHED TO DDC

LASA MAGNITUDE, DMB=MLASA-MNEIS,SECTOR L03

16 EVENTS ARE ANALYZED FROM 65.1 TO 110.0 AZI

EPX NO.	DATE	MNEIS	MLASA	ML-MN	DIST	AZI	DEPTH	BFACTOR
54460	741210	5.00	5.11	0.11	51.3	84.0	33.0	3.40
18425	741120	5.00	5.26	0.26	84.1	100.0	33.0	3.70
98070	740924	5.10	5.12	0.02	60.6	101.0	33.0	3.60
72780	740909	5.00	5.10	0.10	52.4	76.0	33.0	3.40
19575	740812	5.00	5.04	0.04	89.8	90.0	33.0	3.70
50530	740701	5.00	4.98	-0.02	78.9	99.0	33.0	3.50
47391	740627	5.30	5.39	0.09	78.8	99.0	33.0	3.50
46991	740627	5.40	5.48	0.08	78.9	99.0	33.0	3.50
89755	740523	5.10	4.73	-0.37	51.6	89.0	33.0	3.40
77240	740515	5.00	4.47	-0.53	51.5	89.0	33.0	3.40
62975	740507	5.20	4.71	-0.49	61.5	102.0	33.0	3.70
31475	740417	5.10	5.00	-0.10	52.9	75.0	33.0	3.40
6275	740330	5.00	5.28	0.28	76.2	99.0	33.0	3.60
66898	740214	5.40	5.00	-0.40	55.2	94.0	33.0	3.50
6165	740604	5.00	5.37	0.37	64.2	102.0	33.0	3.70
49430	740127	5.10	4.94	-0.16	51.6	78.0	33.0	3.40

THIS PAGE IS BEST QUALITY PRACTICABLE
FROM COPY FURNISHED TO DDC

LASA MAGNITUDE, DMB=MLASA-MNEIS, SECTOR L04

6 EVENTS ARE ANALYZED FROM 110.1 TO 130.0 AZI

EPX NO.	DATE	MNEIS	MLASA	ML-MN	DIST	AZI	DEPTH	BFACTOR
17740	741120	5.20	5.07	-0.13	50.6	113.0	33.0	3.40
47385	741018	5.20	5.48	0.28	46.3	113.0	45.0	3.50
24145	741008	5.10	5.07	-0.03	46.6	113.0	53.0	3.60
66640	740214	5.10	4.89	-0.21	40.0	119.0	7.0	3.10
75895	741029	5.10	5.16	0.06	51.1	120.0	33.0	3.40
40835	740118	5.30	5.02	-0.28	41.0	120.0	82.0	3.20

THIS PAGE IS BEST QUALITY PRACTICABLE
FROM COPY FURNISHED TO DDC

LASA MAGNITUDE, DMB=MLASA-MNEIS, SECTOR L05

97 EVENTS ARE ANALYZED FROM 140.1 TO 160.0 AZI

EPX NO.	DATE	MNEIS	MLASA	ML-MN	DIST	AZI	DEPTH	BFACTOR
66060	741025	5.50	6.38	0.88	32.7	156.0	120.0	3.40
95060	740921	5.30	6.07	0.77	77.8	144.0	106.0	3.60
20746	741007	5.00	4.87	-0.13	64.1	149.0	33.0	3.70
92655	740920	5.00	4.70	-0.30	35.3	153.0	33.0	3.40
15960	740611	5.10	5.43	0.33	82.7	146.0	132.0	3.70
86021	740726	5.00	5.43	0.43	70.5	143.0	157.0	3.60
20600	740409	5.10	5.36	0.26	84.4	150.0	84.0	3.70
47315	741206	5.40	5.61	0.21	43.3	145.0	46.0	3.20
37485	740820	5.40	5.91	0.51	82.3	147.0	93.0	3.60
28785	740816	5.00	5.36	0.36	43.2	144.0	36.0	3.20
90705	741231	5.40	5.65	0.25	34.7	155.0	75.0	3.40
86605	741229	5.50	5.82	0.32	86.1	150.0	99.0	3.60
70720	741217	5.00	5.29	0.29	36.7	150.0	50.0	3.20
62540	741213	5.30	5.66	0.36	73.5	143.0	118.0	3.50
35405	740819	5.20	6.07	0.87	37.3	151.0	67.0	3.20
42120	741204	5.10	5.64	0.54	76.5	145.0	53.0	3.60
38315	741202	5.00	5.64	0.64	82.4	147.0	92.0	3.60
25300	741124	5.00	5.25	0.25	45.9	146.0	36.0	3.50
6550	741114	5.40	5.49	0.09	65.0	148.0	33.0	3.70
2085	741112	5.50	6.08	0.58	86.0	150.0	90.0	3.60
1615	741112	5.00	4.55	-0.45	62.3	149.0	33.0	3.70
93520	741107	5.40	6.25	0.85	69.9	143.0	153.0	3.60
81220	741031	5.20	5.51	0.31	69.5	143.0	83.0	3.60
70505	741026	5.30	5.60	0.30	68.3	145.0	110.0	3.70
38155	741014	5.10	5.14	0.04	55.6	143.0	162.0	3.50
32810	741011	5.10	5.36	0.26	83.6	150.0	65.0	3.70
31180	741011	5.30	5.48	0.18	67.6	146.0	99.0	3.70
30135	741010	5.30	5.34	0.04	64.4	148.0	27.0	3.70
14120	741003	5.00	5.04	0.04	64.5	149.0	33.0	3.70
74879	740911	5.20	5.65	0.45	73.5	143.0	113.0	3.50
60770	740902	5.40	5.87	0.47	79.3	144.0	163.0	3.50
50040	740827	5.50	6.07	0.57	52.7	145.0	147.0	3.70
49055	740827	5.40	4.72	-0.68	89.9	154.0	23.0	3.70
47915	740826	5.10	5.01	-0.09	33.2	152.0	33.0	3.40
45450	740824	5.40	5.24	-0.16	85.6	147.0	32.0	3.60
44085	740824	5.40	5.81	0.41	77.1	144.0	109.0	3.60
6510	740928	5.00	5.56	0.56	46.2	146.0	33.0	3.50
63415	740507	5.00	5.19	0.19	43.1	144.0	33.0	3.20
80430	740516	5.50	5.58	0.08	39.3	147.0	36.0	3.10
8305	740606	5.10	5.36	0.26	76.2	144.0	116.0	3.60
11720	740608	5.00	5.59	0.59	77.3	144.0	106.0	3.60
13320	740609	5.10	4.66	-0.44	57.0	149.0	52.0	3.50
50855	740701	5.50	5.49	-0.01	78.3	141.0	13.0	3.60
62095	740710	5.00	5.24	0.24	78.0	144.0	121.0	3.60
73600	740717	5.20	5.50	0.30	80.8	148.0	33.0	3.50
76485	740719	5.20	4.96	-0.24	85.3	151.0	44.0	3.70
79920	740721	5.00	4.89	-0.11	39.4	147.0	78.0	3.10
33335	740818	5.30	5.44	0.14	92.6	157.0	21.0	3.90
28425	740102	5.30	5.26	-0.04	77.3	144.0	99.0	3.60
33935	740107	5.10	5.00	-0.10	85.6	151.0	24.0	3.60
39675	740117	5.30	5.66	0.36	81.4	148.0	83.0	3.50
43785	740121	5.00	5.26	0.26	33.5	157.0	33.0	3.40
54980	740201	5.20	5.42	0.22	68.4	147.0	48.0	3.70
55700	740202	5.10	5.40	0.30	34.7	155.0	75.0	3.40
56515	740202	5.20	5.41	0.21	68.8	147.0	63.0	3.70
66405	740214	5.00	4.98	-0.02	81.2	144.0	33.0	3.50
68811	740216	5.30	5.70	0.40	75.5	145.0	74.0	3.60
72155	740220	5.50	5.84	0.34	83.9	147.0	115.0	3.70
73430	740221	5.10	5.81	0.71	87.8	151.0	87.0	3.80
79995	740228	5.20	4.63	-0.57	41.9	146.0	59.0	3.20
88720	740310	5.10	4.64	-0.46	51.6	145.0	43.0	3.40

THIS PAGE IS BEST QUALITY PRACTICABLE
FROM COPY FURNISHED TO DDC

LASA MAGNITUDE, DMB=MLASA-MNEIS, SECTOR L05

97 EVENTS ARE ANALYZED FROM 140.1 TO 160.0 AZI

EPX NO.	DATE	MNEIS	MLASA	ML-MN	DIST	AZI	DEPTH	BFACTOR
89482	740311	5.10	5.26	0.16	61.3	148.0	97.0	3.60
945	740324	5.30	5.67	0.37	86.0	150.0	104.0	3.60
7605	740331	5.00	5.20	0.20	38.2	150.0	49.0	3.20
9570	740402	5.50	5.86	0.36	85.9	145.0	166.0	3.60
27485	740414	5.30	4.90	-0.40	34.3	153.0	138.0	3.40
43920	740425	5.30	5.29	-0.01	71.3	144.0	33.0	3.60
45520	740426	5.50	5.63	0.13	78.8	145.0	97.0	3.50
7020	740331	5.20	5.39	0.19	82.7	177.0	33.0	3.70
28355	741008	5.00	4.72	-0.28	55.8	148.0	33.0	3.50
42610	740823	5.40	5.72	0.32	79.7	146.0	102.0	3.40
4460	740804	5.20	5.47	0.27	78.4	146.0	68.0	3.60
45680	740123	5.20	5.73	0.53	85.4	149.0	115.0	3.70
33115	740107	5.30	5.63	0.33	82.7	149.0	35.0	3.70
80015	740721	5.00	5.20	0.20	39.3	147.0	87.0	3.10
14880	740810	5.20	5.45	0.25	75.5	143.0	116.0	3.60
79252	740721	5.30	5.34	0.04	34.5	155.0	70.0	3.40
22160	740410	5.40	5.31	-0.09	34.4	154.0	108.0	3.40
15321	741004	5.00	5.06	0.06	79.3	140.0	533.0	3.50
70205	740907	5.20	4.67	-0.53	89.8	155.0	16.0	3.70
21555	741007	5.10	5.07	-0.03	39.2	146.0	225.0	3.10
73820	741224	5.40	6.25	0.85	35.1	152.0	155.0	3.40
65965	740905	5.40	5.84	0.44	49.0	133.0	160.0	3.50
59895	740206	5.10	5.44	0.34	48.9	133.0	160.0	3.50
71435	740715	5.30	5.28	-0.02	46.2	138.0	28.0	3.50
68250	740714	5.20	5.33	0.13	45.9	138.0	26.0	3.50
67485	740713	5.40	5.38	-0.02	46.0	138.0	5.0	3.50
65206	740713	5.50	5.57	0.07	46.3	138.0	45.0	3.50
65165	740713	5.20	5.25	0.05	46.1	138.0	23.0	3.50
65100	740713	5.30	5.66	0.36	46.1	138.0	24.0	3.50
51266	740429	5.10	5.41	0.31	49.3	138.0	87.0	3.50
3775	740602	5.20	5.53	0.33	48.5	139.0	64.0	3.50
56100	740705	5.20	4.96	-0.24	37.9	139.0	23.0	3.20
64835	740713	5.40	5.39	-0.01	46.1	139.0	33.0	3.50
64875	740713	5.20	5.11	-0.09	46.6	139.0	21.0	3.60
65266	740713	5.10	4.96	-0.14	46.2	139.0	33.0	3.50
67955	740713	5.30	5.47	0.17	46.5	139.0	23.0	3.60

THIS PAGE IS BEST QUALITY PRACTICABLE
FROM COPY FURNISHED TO DDC

LASA MAGNITUDE, DMB=MLASA-MNEIS,SECTOR L06

20 EVENTS ARE ANALYZED FROM 160.1 TO 210.0 AZI

EPX NO.	DATE	MNEIS	MLASA	ML-MN	DIST	AZI	DEPTH	BFACTOR
30830	740105	5.00	4.69	-0.31	38.4	176.0	33.0	3.20
32795	740107	5.40	5.77	0.37	48.4	160.0	33.0	3.60
48275	740126	5.10	4.63	-0.47	28.2	174.0	33.0	3.30
34140	740418	5.10	5.06	-0.04	85.7	170.0	33.0	3.60
34345	740408	5.50	5.58	0.08	85.6	170.0	33.0	3.60
48675	740428	5.10	5.17	0.07	50.6	177.0	33.0	3.40
62325	740506	5.00	4.86	-0.14	77.6	183.0	33.0	3.60
17500	740612	5.00	5.16	0.16	30.4	166.0	49.0	3.30
19640	740613	5.00	4.98	-0.02	30.7	164.0	96.0	3.20
43370	740625	5.30	5.09	-0.21	32.5	160.0	25.0	3.40
55440	740705	5.20	4.32	-0.88	94.3	161.0	33.0	3.80
57010	740706	5.10	5.01	-0.09	81.7	181.0	33.0	3.60
85020	740725	5.30	5.65	0.35	73.7	187.0	33.0	3.50
20180	740812	5.10	4.90	-0.20	29.5	168.0	73.0	3.30
59085	740901	5.00	4.99	-0.01	92.1	163.0	33.0	3.80
20155	741006	5.00	5.13	0.13	30.3	167.0	51.0	3.30
31625	741011	5.00	4.78	-0.22	60.2	186.0	33.0	3.50
87101	741103	5.10	5.32	0.22	81.5	181.0	33.0	3.50
40240	741203	5.20	5.39	0.19	72.5	189.0	33.0	3.60
67970	741216	5.10	5.23	0.13	71.8	185.0	33.0	3.60

THIS PAGE IS BEST QUALITY PRACTICABLE
FROM COPY FURNISHED TO DDC

LASA MAGNITUDE, DMB=MLASA-MNEIS, SECTOR L07

24 EVENTS ARE ANALYZED FROM 210.1 TO 250.0 AZI

EPX NO.	DATE	MNEIS	MLASA	ML-MN	DIST	AZI	DEPTH	BFACTOR
45075	740123	5.40	5.39	-0.01	95.6	242.0	449.0	3.60
79770	740228	5.30	4.60	-0.70	89.5	241.0	98.0	3.60
340	740323	5.30	5.63	0.33	91.5	240.0	33.0	3.80
81970	740517	5.30	4.92	-0.38	98.8	240.0	494.0	3.90
3235	740602	5.30	4.85	-0.45	87.1	241.0	7.0	3.70
3957	740603	5.40	5.81	0.41	93.0	242.0	33.0	3.90
33160	740620	5.30	4.98	-0.32	98.9	241.0	540.0	3.90
33860	740620	5.40	5.19	-0.21	86.3	243.0	31.0	3.60
46135	740626	5.40	5.09	-0.31	97.3	242.0	551.0	3.70
69470	740714	5.30	4.25	-1.05	99.0	237.0	183.0	3.90
77160	740719	5.30	4.85	-0.45	86.1	241.0	33.0	3.60
81715	740723	5.50	5.35	-0.15	87.4	242.0	46.0	3.70
83210	740724	5.40	5.20	-0.20	101.1	235.0	33.0	4.10
15030	740810	5.50	5.37	-0.13	94.4	243.0	602.0	3.60
47185	740825	5.30	4.95	-0.35	96.5	242.0	542.0	3.70
52515	740829	5.30	5.10	-0.20	99.1	237.0	58.0	4.10
93135	740920	5.30	5.38	0.08	94.3	239.0	33.0	3.80
38830	741014	5.30	3.87	-1.43	93.3	242.0	554.0	3.50
49140	741018	5.40	5.28	-0.12	86.5	241.0	33.0	3.70
95510	741108	5.30	5.21	-0.09	86.4	242.0	12.0	3.60
95520	741108	5.40	5.56	0.16	86.4	242.0	33.0	3.60
23430	741123	5.40	4.96	-0.44	94.5	241.0	211.0	3.70
93875	740729	5.40	5.76	0.36	91.4	245.0	586.0	3.50
21950	740813	5.40	5.03	-0.37	90.5	247.0	55.0	3.70

THIS PAGE IS BEST QUALITY PRACTICABLE
FROM COPY FURNISHED TO DDC

LASA MAGNITUDE, DMB=MLASA-MNEIS,SECTOR L08

17 EVENTS ARE ANALYZED FROM 250.1 TO 290.0 AZI

EPX NO.	DATE	MNEIS	MLASA	ML-MN	DIST	AZI	DEPTH	BFACTOR
43296	740121	5.40	5.52	0.12	98.5	266.0	38.0	4.20
54240	740201	5.40	5.05	-0.35	100.8	270.0	33.0	4.00
55400	740201	5.40	4.92	-0.48	101.0	271.0	47.0	4.00
57355	740203	5.40	4.91	-0.49	101.0	270.0	43.0	4.00
58365	740204	5.40	4.73	-0.67	100.7	270.0	55.0	4.10
63060	740210	5.40	4.85	-0.55	101.2	271.0	38.0	4.00
8845	740402	5.40	5.20	-0.20	100.8	271.0	47.0	4.10
58895	740504	5.50	5.44	-0.06	94.1	254.0	602.0	3.60
12470	740608	5.40	5.50	0.10	99.0	265.0	34.0	4.20
18140	740612	5.40	5.25	-0.15	99.3	265.0	33.0	4.20
85160	740725	5.50	5.19	-0.31	101.7	273.0	33.0	4.10
22185	740813	5.50	5.41	-0.09	102.7	275.0	100.0	4.30
25340	740815	5.50	5.63	0.13	99.7	267.0	59.0	4.10
1055	740925	5.40	5.45	0.05	106.5	273.0	10.0	4.60
14895	741119	5.50	4.60	-0.90	101.3	277.0	18.0	4.00
49650	741207	5.40	4.96	-0.44	100.5	272.0	93.0	4.10
91080	741231	5.50	6.07	0.57	48.6	252.0	5.0	3.50

THIS PAGE IS BEST QUALITY PRACTICABLE
FROM COPY FURNISHED TO DDC

LASA MAGNITUDE, DMB=MLASA-MNEIS,SECTOR L09

151 EVENTS ARE ANALYZED FROM 290.1 TO 325.0 AZI

EPX NO.	DATE	MNEIS	MLASA	ML-MN	DIST	AZI	DEPTH	BFACTOR
37915	740622	5.20	4.74	-0.46	73.8	311.0	40.0	3.50
38740	740622	5.10	5.11	0.01	87.9	295.0	103.0	3.50
46370	740627	5.00	4.38	-0.62	85.1	313.0	39.0	3.70
58655	740707	5.20	5.24	0.04	64.0	311.0	33.0	3.70
66645	740713	5.10	5.11	0.01	93.0	315.0	97.0	3.80
90050	740728	5.00	5.14	0.14	63.8	310.0	60.0	3.40
95215	740730	5.00	4.89	-0.11	64.0	310.0	42.0	3.50
98160	740801	5.20	4.74	-0.46	29.6	306.0	33.0	3.30
99285	740801	5.00	4.63	-0.37	87.6	299.0	321.0	3.40
46840	740825	5.00	5.01	0.01	80.0	306.0	33.0	3.40
50685	740828	5.00	4.74	-0.26	77.3	310.0	51.0	3.50
56800	740830	5.30	5.03	-0.27	81.3	306.0	24.0	3.50
56195	740830	5.10	4.27	-0.83	81.4	306.0	46.0	3.40
61845	740903	5.30	4.98	-0.32	79.9	306.0	20.0	3.40
63440	740903	5.00	4.60	-0.40	79.9	306.0	15.0	3.40
65890	740905	5.10	4.97	-0.13	79.8	306.0	33.0	3.40
71630	740908	5.10	5.27	0.17	86.9	299.0	135.0	3.50
85735	740916	5.30	5.01	-0.29	67.6	311.0	54.0	3.50
86010	740917	5.00	4.50	-0.50	29.2	306.0	17.0	3.30
16505	741004	5.00	4.45	-0.55	56.7	313.0	33.0	3.50
33795	741012	5.30	5.32	0.02	73.0	311.0	26.0	3.60
39835	741015	5.40	4.98	-0.42	72.8	311.0	22.0	3.60
40240	741015	5.00	4.80	-0.20	67.7	311.0	79.0	3.30
64515	741024	5.10	4.20	-0.90	81.3	306.0	45.0	3.40
79700	741030	5.30	5.50	0.20	88.0	313.0	33.0	3.80
79885	741030	5.00	4.86	-0.14	85.3	304.0	422.0	3.30
84725	741102	5.10	4.60	-0.50	73.0	313.0	67.0	3.30
85810	741102	5.10	4.54	-0.56	77.1	310.0	44.0	3.60
92950	741107	5.00	5.42	0.42	69.5	312.0	55.0	3.50
97995	741109	5.40	4.69	-0.71	73.4	311.0	27.0	3.60
670	741111	5.00	5.05	0.05	89.6	313.0	44.0	3.70
12180	741117	5.00	4.52	-0.48	72.5	312.0	42.0	3.60
30795	741128	5.30	4.75	-0.55	36.4	302.0	32.0	3.30
43705	741205	5.00	4.58	-0.42	88.4	295.0	185.0	3.30
45390	741205	5.00	4.91	-0.09	81.0	305.0	33.0	3.50
55730	741210	5.00	4.98	-0.02	70.0	311.0	36.0	3.60
64200	741213	5.00	4.58	-0.42	62.9	311.0	33.0	3.60
76845	741225	5.10	5.51	0.41	49.4	306.0	37.0	3.50
89125	741231	5.10	5.31	0.21	45.6	305.0	228.0	2.90
62885	740507	5.00	4.40	-0.60	96.6	316.0	36.0	4.10
59905	740505	5.50	4.85	-0.65	98.7	316.0	26.0	4.20
25383	740412	5.50	5.49	-0.01	98.5	301.0	33.0	4.20
38615	740116	5.10	4.24	-0.86	97.7	316.0	58.0	4.00
56255	740502	5.00	4.91	-0.09	78.2	309.0	33.0	3.60
16970	741004	5.30	4.56	-0.74	56.6	312.0	16.0	3.50
97410	740801	5.20	4.49	-0.71	29.6	306.0	10.0	3.30
8810	740402	5.20	5.26	0.06	73.4	313.0	41.0	3.60
97905	740322	5.10	5.13	0.03	36.2	302.0	33.0	3.30
6680	740806	5.00	4.52	-0.48	30.3	313.0	136.0	3.20
24105	741123	5.40	5.25	-0.15	96.5	315.0	33.0	4.10
41620	740823	5.00	4.75	-0.25	97.3	316.0	33.0	4.10
12615	740808	5.40	4.92	-0.48	96.1	316.0	32.0	4.00
26215	740617	5.10	5.05	-0.05	62.1	311.0	33.0	3.70
49280	740127	5.30	5.18	-0.12	87.1	298.0	148.0	3.40
61005	740505	5.10	4.99	-0.11	66.1	312.0	143.0	3.30
30955	740105	5.40	5.40	0.00	41.3	302.0	41.0	3.20
77205	740415	5.00	4.73	-0.27	39.7	302.0	44.0	3.10
38755	741014	5.30	4.45	-0.85	72.9	311.0	15.0	3.60
54290	741020	5.30	5.40	0.10	72.3	313.0	24.0	3.60
64260	741024	5.40	5.42	0.02	79.8	308.0	63.0	3.40
71140	741027	5.10	5.34	0.24	69.1	314.0	223.0	3.20

THIS PAGE IS BEST QUALITY PRACTICABLE
FROM COPY FURNISHED TO DDC

LASA MAGNITUDE, DMB=MLASA-MNEIS, SECTOR L09

151 EVENTS ARE ANALYZED FROM 290.1 TO 325.0 AZI

EPX NO.	DATE	MNEIS	MLASA	ML-MN	DIST	AZI	DEPTH	BFACTOR
5060	741114	5.50	5.86	0.36	30.9	310.0	37.0	3.40
12460	741117	5.30	5.17	-0.13	54.6	315.0	31.0	3.50
16660	741120	5.00	5.23	0.23	37.3	302.0	57.0	3.30
29675	741128	5.20	5.61	0.41	43.6	303.0	63.0	3.20
34345	741130	5.20	5.42	0.22	49.5	309.0	17.0	3.40
21075	741007	5.20	5.52	0.32	69.2	315.0	325.0	3.20
12275	741002	5.20	5.39	0.19	58.1	313.0	51.0	3.50
85805	740916	5.50	5.95	0.45	60.4	312.0	48.0	3.50
61915	740903	5.20	5.70	0.50	60.3	312.0	22.0	3.50
46245	740825	5.30	5.29	-0.01	80.0	306.0	40.0	3.40
32960	740818	5.00	5.42	0.42	49.6	305.0	33.0	3.40
55	740801	5.30	5.73	0.43	60.3	312.0	41.0	3.60
87175	741230	5.10	5.37	0.27	28.8	317.0	62.0	3.10
34000	741012	5.50	5.44	-0.06	73.0	311.0	24.0	3.60
40550	741203	5.00	5.32	0.32	62.5	312.0	36.0	3.60
64740	740904	5.30	4.93	-0.37	74.1	312.0	55.0	3.40
46735	740825	5.20	5.04	-0.16	80.0	306.0	81.0	3.30
45705	740824	5.70	4.65	-1.05	39.4	301.0	37.0	3.10
37860	740421	5.30	5.56	0.26	67.9	314.0	28.0	3.70
33710	740418	5.00	5.51	0.51	54.1	313.0	46.0	3.50
34580	740819	5.30	5.38	0.08	80.5	309.0	23.0	3.50
23515	740814	5.30	5.49	0.19	72.9	312.0	41.0	3.60
7695	740806	5.20	4.81	-0.39	65.0	312.0	166.0	3.20
23985	740411	5.30	5.12	-0.18	71.1	312.0	75.0	3.30
20910	740409	5.20	5.34	0.14	86.2	295.0	43.0	3.50
20785	740409	5.50	5.77	0.27	67.0	312.0	139.0	3.40
12020	740404	5.30	5.28	-0.02	76.5	311.0	97.0	3.30
95315	740319	5.00	4.94	-0.06	78.4	309.0	58.0	3.30
4630	740805	5.10	5.34	0.24	42.4	303.0	66.0	3.30
92890	740315	5.00	5.42	0.42	59.2	311.0	35.0	3.50
86840	740308	5.50	5.76	0.26	86.5	313.0	42.0	3.70
74915	740223	5.30	5.07	-0.23	72.0	313.0	64.0	3.30
91455	740729	5.00	5.31	0.31	63.8	311.0	54.0	3.50
90880	740728	5.10	5.37	0.27	64.0	310.0	52.0	3.50
24750	741008	5.00	4.58	-0.42	78.2	311.0	56.0	3.30
48190	740126	5.30	5.50	0.20	41.2	302.0	54.0	3.30
41590	740119	5.00	5.12	0.12	39.1	302.0	59.0	3.30
62015	740208	5.40	5.38	-0.02	51.8	312.0	33.0	3.40
61260	740207	5.00	5.56	0.56	59.9	312.0	46.0	3.50
58621	740205	5.00	5.19	0.19	28.6	319.0	75.0	3.10
90541	740728	5.40	5.81	0.41	63.9	310.0	46.0	3.70
90491	740728	5.30	5.24	-0.06	63.8	310.0	66.0	3.40
90165	740728	5.30	5.46	0.16	64.0	310.0	46.0	3.70
87771	740727	5.30	5.66	0.36	51.9	314.0	33.0	3.40
73675	740717	5.00	5.11	0.11	42.7	302.0	45.0	3.20
43300	740625	5.50	5.17	-0.33	87.2	298.0	173.0	3.30
42476	740624	5.30	5.60	0.30	82.2	310.0	393.0	3.20
95150	740527	5.50	5.25	-0.25	26.7	315.0	21.0	3.10
39650	740623	5.00	4.80	-0.20	39.8	302.0	42.0	3.10
9870	740607	5.00	4.81	-0.19	41.2	300.0	33.0	3.20
50325	740429	5.10	4.95	-0.15	86.1	296.0	33.0	3.60
47790	740427	5.00	4.98	-0.02	53.4	315.0	26.0	3.40
44590	740425	5.00	4.79	-0.21	87.3	312.0	33.0	3.70
37275	740420	5.10	4.83	-0.27	71.9	313.0	66.0	3.40
28180	740414	5.10	4.71	-0.39	92.2	312.0	33.0	3.80
27970	740414	5.10	4.70	-0.40	92.1	312.0	33.0	3.80
8700	740401	5.30	5.37	0.07	81.0	306.0	16.0	3.50
3610	740327	5.00	4.19	-0.81	72.7	312.0	53.0	3.30
96880	740321	5.30	5.19	-0.11	76.6	310.0	43.0	3.60
96630	740320	5.00	4.51	-0.49	81.0	308.0	77.0	3.30

THIS PAGE IS BEST QUALITY PRACTICABLE
FROM COPY FURNISHED TO DDC

LASA MAGNITUDE, DMB=MLASA-MNEIS,SECTOR L09

151 EVENTS ARE ANALYZED FROM 290.1 TO 325.0 AZI

EPX NO.	DATE	MNEIS	MLASA	ML-MN	DIST	AZI	DEPTH	BFACTOR
94990	740318	5.10	5.18	0.08	92.3	314.0	140.0	3.80
94305	740317	5.20	5.31	0.11	91.2	313.0	74.0	3.70
90485	740312	5.00	4.52	-0.48	88.2	314.0	80.0	3.50
85611	740306	5.00	4.83	-0.17	73.8	312.0	59.0	3.30
85025	740306	5.00	4.96	-0.02	68.1	311.0	33.0	3.70
79925	740228	5.00	4.48	-0.52	38.3	302.0	33.0	3.20
63411	740210	5.00	4.63	-0.37	80.5	312.0	55.0	3.30
56210	740202	5.10	4.80	-0.30	27.8	317.0	48.0	3.20
47216	740125	5.00	4.59	-0.41	71.8	312.0	41.0	3.60
46840	740124	5.20	5.04	-0.16	71.7	312.0	41.0	3.60
46191	740124	5.20	5.28	0.08	86.1	301.0	33.0	3.60
38111	740111	5.10	5.00	-0.10	81.0	306.0	20.0	3.50
36435	740110	5.20	5.09	-0.11	85.8	313.0	37.0	3.60
36275	740110	5.10	4.98	-0.12	77.1	310.0	47.0	3.60
35775	740110	5.30	4.58	-0.72	57.3	312.0	33.0	3.50
35025	740109	5.40	4.77	-0.63	57.3	312.0	33.0	3.50
28935	740103	5.10	5.43	0.33	87.2	297.0	139.0	3.70
27075	740101	5.00	4.67	-0.33	87.7	299.0	333.0	3.40
37035	741202	5.50	5.43	-0.07	101.6	314.0	53.0	4.10
67715	740510	5.00	4.27	-0.73	90.3	312.0	33.0	3.70
79995	740516	5.30	4.73	-0.57	85.0	305.0	471.0	3.10
92155	740524	5.00	4.81	-0.19	56.4	313.0	33.0	3.50
95	740531	5.10	4.66	-0.44	56.3	313.0	33.0	3.50
27045	740617	5.00	4.68	-0.32	72.9	312.0	60.0	3.30
56255	740502	5.00	4.91	-0.09	78.2	309.0	33.0	3.60
49980	740128	5.50	5.44	-0.06	94.9	293.0	58.0	3.90
77395	740226	5.50	5.48	-0.02	94.4	293.0	45.0	3.80
84235	740724	5.40	5.70	0.30	93.0	292.0	78.0	3.80
38875	740422	5.20	4.96	-0.24	91.6	322.0	33.0	3.80
30035	740817	5.40	5.50	0.10	62.5	322.0	1.0	3.70

THIS PAGE IS BEST QUALITY PRACTICABLE
FROM COPY FURNISHED TO DDC

IASP MAGNITUDE, DMD=MLASA-MNEIS,SECTOR L10

7 EVENTS ARE ANALYZED FROM 325.1 TO 350.0 AZI

EPX NO.	DATE	MNEIS	MLASA	ML-MN	DIST	AZI	DEPTH	BFACTOR
38420	740115	5.30	5.19	-0.11	95.8	334.0	33.0	3.90
98285	740322	5.50	5.65	0.15	82.3	349.0	33.0	3.60
7250	740605	5.20	4.89	-0.31	100.2	333.0	33.0	4.10
36280	740621	5.30	5.31	0.01	70.6	336.0	33.0	3.60
55085	740704	5.10	4.76	-0.34	86.5	345.0	33.0	3.70
97315	740923	5.10	5.05	-0.05	95.7	336.0	33.0	4.00
10525	741116	5.10	4.83	-0.27	95.7	334.0	33.0	4.00

APPENDIX B

Signal Variance Among Sources and Receivers as a Consequence of the Seismic Reciprocity Theorem

From Knopoff and Gangi (1959), the seismic reciprocity theorem for linear elasticity is

$$u_i(P,Q)\ f_i(P) = u_j(Q,P)\ f_j(Q)$$

where $u_i(P,Q)$ is the i component of displacement at receiver point P due to source at Q of strength $f_j(Q)$ in the direction j. The theorem is valid in inhomogeneous, non-isotropic media with arbitrary boundaries.

In this form the theorem is not suited for applications to problems of magnitude-yield because an explosion source is not a directed force, but rather a dilatation expanding against hydrostatic pressure. The relevant generalization is (Knopoff, 1978 personal communication)

$$\nabla\cdot u(P,Q)\ \tau(P) = \nabla\cdot u(Q,P)\ \tau(Q)$$

Verbally, this equation can be expressed as: a unit dilatation at Q working against hydrostatic pressure $\tau(Q)$ produces a divergence at P that when multiplied by $\tau(P)$ is equal to the divergence produced at Q by a unit dilatation at P multiplied by $\tau(Q)$.

Again, this theorem is valid in inhomogenous, non-isotropic media with arbitrary boundaries.

Explosions of equal yield at equal depth should satisfy the condition of equal dilatations at equal pressures. Thus in applying this to the present study, if the divergence (of a signal from Semipalatinsk) could be measured at a shot depth at subarrays of LASA; the variance of the divergence measurements would be equal to the variance observed in the divergence measured at shot depth near the shot at Semipalatinsk from a series of explosions set off at the subarrays of LASA.

The only problem here is that in practice we measure displacements at the surface, not divergence at shot depth. However, to the extent that the incoming wave at both LASA and Semipalatinsk can be modelled as a plane wave the divergence may be simply calculated as the vertical derivative of the incoming wave amplitude with a delayed signal of the same polarity (the reflection from the surface). If focussing and de-focussing are the main causes of signal amplitude variation, then the maximum divergence at depth will be a constant

factor times the maximum displacement at the surface. Thus, the variance of the divergence in logarithmic units will be the same as the variance of the displacement. Thus, finally, the variance of the displacement at Semipalatinsk from shots spaced around LASA will be equal to the variance observed at the shotpoints from a shot at Semipalatinsk.

In this report variance measurements have been made at LASA on the signals from earthquakes, not explosions. Thus, while the theorem is not totally valid, we can see that our conclusions about variance are still valid. Consider that the P-wave signal, as it emerges from the earthquake, could have come from an explosion of suitably determined yield. In logarithmic units this factor would cancel out of variance estimates so that we could predict the variance to be observed at the earthquake foci from shots spaced around LASA. Since the crust above the earthquake, between the earthquake and a surface sensor, is a complex part of the path, the variance observed at the surface would then be greater than, or equal to, the variance observed at LASA from the earthquakes. This conclusion applies only so long as the radiation patterns of the earthquakes do not vary significantly across LASA.

Note also that the variance observed at RKON due to shots spaced around the Nevada Test Site (NTS) is equal to the variance that would be observed at NTS from a shot at RKON. Or, another example, the variance observed at NTS from a shot at Semipalatinsk is equal to the variance which would be observed at Semipalatinsk from shots spaced around NTS. Clearly, there are many applications of this theorem.

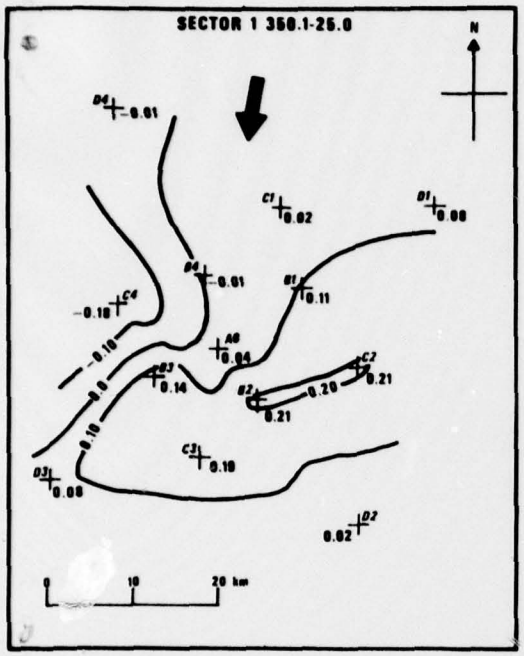
SECTOR 1 350.1-25.0
N
0 10 20 km

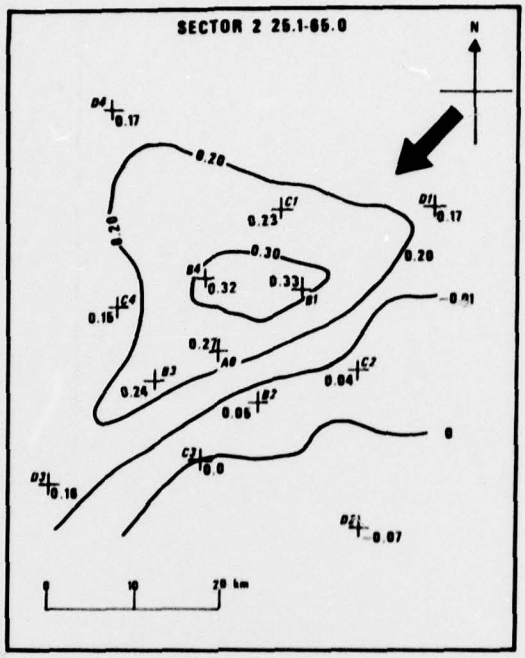
SECTOR 2 25.1-65.0
N
0 10 20 km

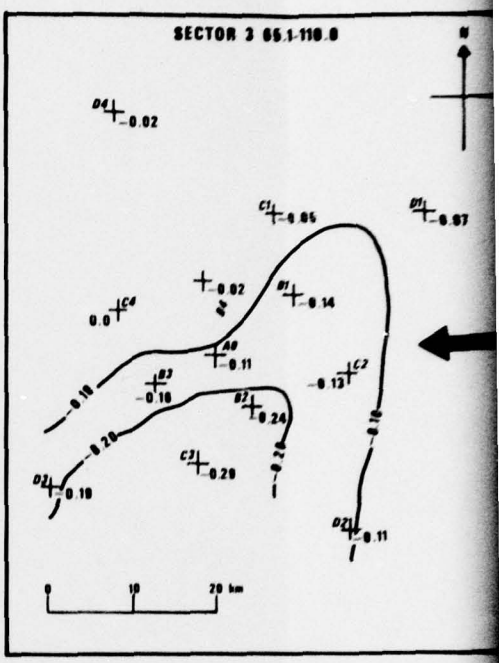
SECTOR 3 65.1-110.0
N
0 10 20 km

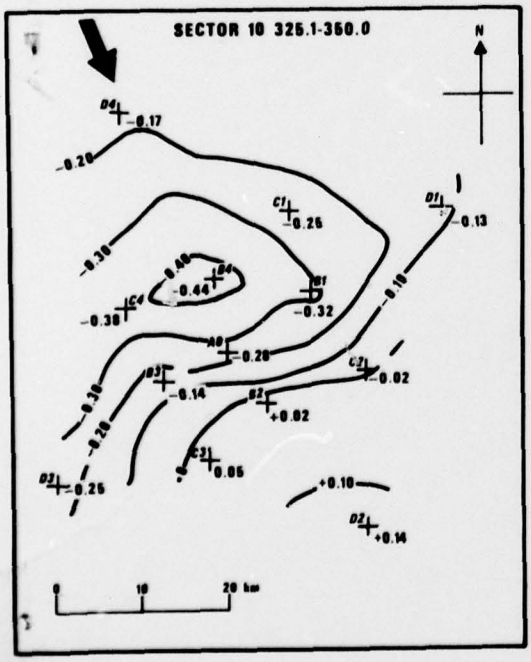
SECTOR 10 325.1-350.0
N
0 10 20 km

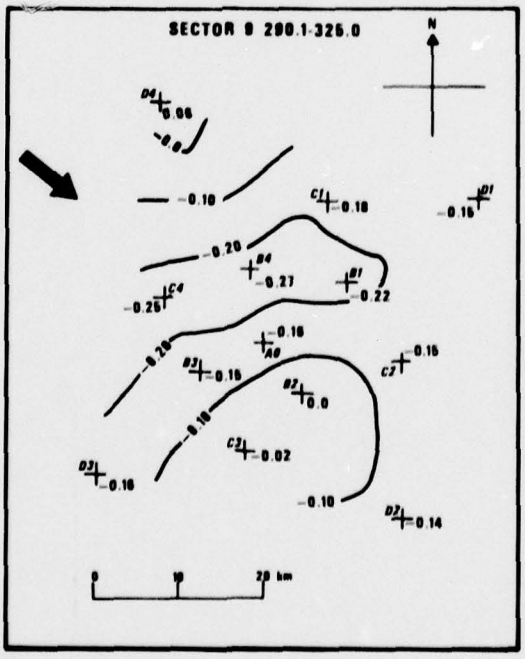
SECTOR 9 290.1-325.0
N
0 10 20 km

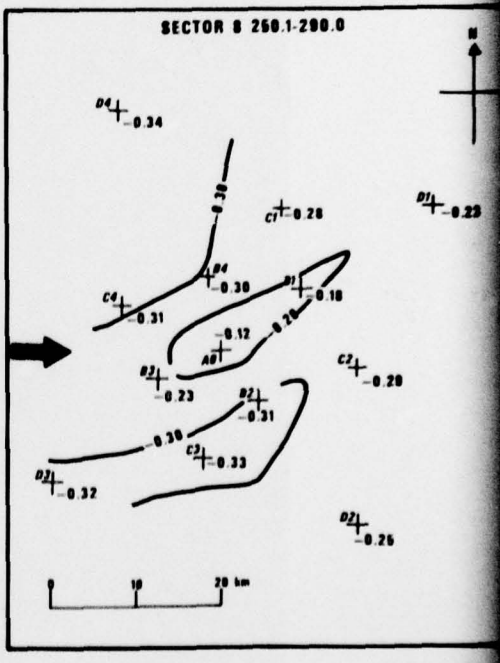
SECTOR 8 250.1-290.0
N
0 10 20 km


N

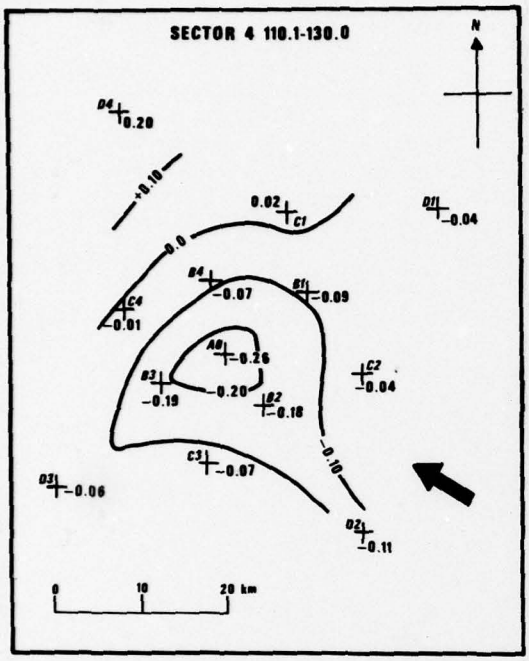
SECTOR 4 110.1-130.0
N
D4 0.20
+0.10
0.02 C1
D1 -0.04
0.0
B4 -0.07
B1 -0.09
C4 -0.01
A0 -0.26
B3 -0.19
-0.20
B2 -0.18
C2 -0.04
C3 -0.07
-0.10
D3 -0.06
D2 -0.11
0 10 20 km

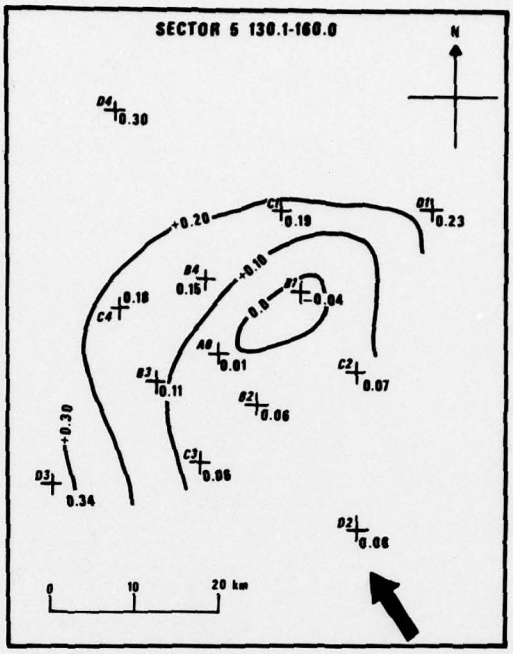
SECTOR 5 130.1-160.0
N
D4 0.30
+0.20
C1 0.19
D1 0.23
B4 0.15
+0.10
D1 -0.04
C4 0.18
0.0
A0 0.01
C2 0.07
B3 0.11
B2 0.06
+0.30
C3 0.06
D3 0.34
D2 0.08
0 10 20 km


N

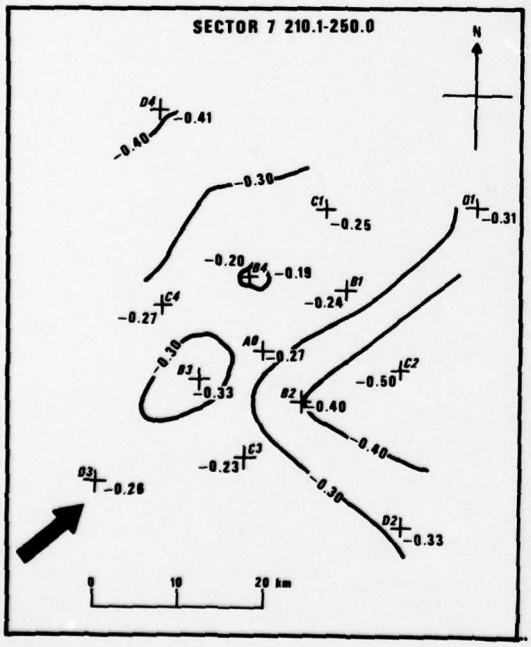
SECTOR 7 210.1-250.0
N
D4 -0.41
-0.40
-0.30
C1 -0.25
D1 -0.31
-0.20
B4 -0.19
B1 -0.24
C4 -0.27
-0.30
A0 -0.27
B3 -0.33
C2 -0.50
B2 -0.40
-0.40
C3 -0.23
-0.30
D3 -0.26
D2 -0.33
0 10 20 km

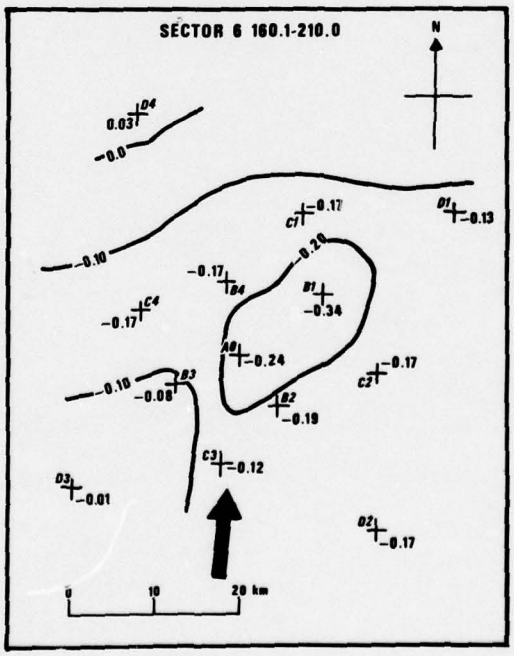
SECTOR 6 160.1-210.0
N
D4 0.03
-0.0
C1 -0.17
D1 -0.13
-0.10
-0.17
B4
B1 -0.34
C4 -0.17
-0.20
A0 -0.24
C2 -0.17
-0.10
B3 -0.08
B2 -0.19
C3 -0.12
D3 -0.01
D2 -0.17
0 10 20 km